4. Passive Microwave Devices

4.1 Periodic Structures

Waveguides and transmission lines loaded at periodic intervals with reactive elements such as diaphragms and stubs are referred to as periodic structures. The interest in waveguiding structures of this type arises from some basic properties common to all periodic structures, namely, (a) passband-stopband characteristics (b) propagation characteristics like fast wave, slow wave, forward wave, backward wave and (c) applications for design of filters, EBG structures, leaky-wave antennas, traveling-wave tubes, DNG metamaterials, etc.

- **Phase and group velocity**

Phase velocity of a wave is the rate at which phase of wave propagates in space. This is the velocity at which phase of any one frequency component of the wave will propagate. In mathematical terms, ω be the angular frequency and β is the phase constant. Then phase velocity v_p is defined as $v_p=\omega/\beta$. The group velocity of a wave is the velocity with which the overall shape of wave amplitude (known as the envelope of the wave) propagates through space. The group velocity is the velocity with which energy propagates and is defined by $v_g = \frac{\partial \omega}{\partial \beta}$. The phase velocity is also given by the slope of a line from origin to a point on dispersion curve, while the group velocity is given by slope of a tangent to the dispersion curve.

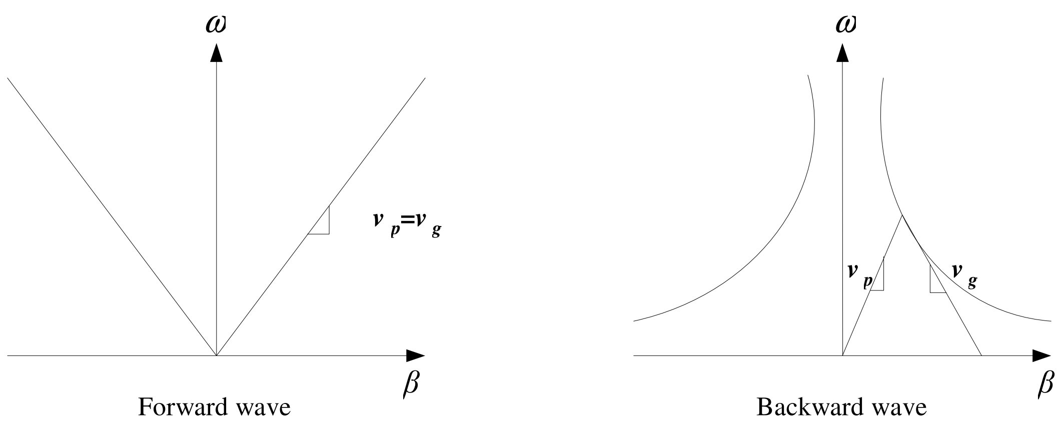

Figure 4.1: Dispersion curve

- **Forward and backward wave**

Dispersive propagation occurs when phase velocity depends on frequency. Most of our acquaintance with the waves is non dispersive propagation, in which phase velocity is independent of frequency. For forward wave, phase and group velocity are constant and equal to one another. This simple relation does not hold in general. Backward wave, in which phase velocity is opposite in direction of propagation to group velocity is very counter-intuitive concept. But, they are simply a normal phenomenon that occurs with some of the dispersive propagation.

- **Forward wave transmission line**

Let us consider the simplified distributed equivalent circuit of conventional transmission line as illustrated in Figure 4.2. It consists of series inductance and shunt capacitance in the LC ladder network. For such a lossless line, $\gamma = j\beta = \sqrt{ZY} = \sqrt{j\omega L j\omega C} = j\omega\sqrt{LC}$ is the propagation constant. Here, $v_p = \frac{\omega}{\beta} = \frac{1}{\sqrt{LC}}$ and $v_g = \frac{\partial\omega}{\partial\beta} = \frac{1}{\sqrt{LC}}$. Hence, wave packet travels at the same speed and direction with the phase velocity.

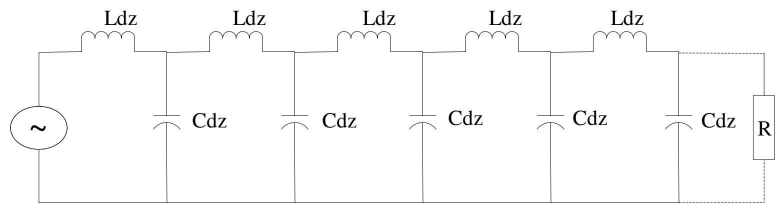

Figure 4.2: Forward wave transmission line $(Z = j\omega L; Y = j\omega C)$

- **Backward wave transmission line**

Consider the backward wave transmission line as shown in Figure 4.3. It consists of series capacitor and shunt inductor in the LC ladder network. Hence, it is a high-pass lossless line unlike the forward-wave lossless line we considered before, which is a low-pass line. The dispersion relation is given by $\gamma = j\beta = \sqrt{ZY} = \sqrt{\frac{1}{j\omega C}\frac{1}{j\omega L}} = \frac{-j}{\omega\sqrt{LC}}$ or $v_p = \frac{\omega}{\beta} = -\omega^2\sqrt{LC}$. This line is strongly dispersive. $v_g = \frac{\partial\omega}{\partial\beta} = \frac{1}{\frac{\partial\beta}{\partial\omega}} = \omega^2\sqrt{LC}$, is negative of the phase velocity. The wavelets in a wave packet appear to travel in a direction opposite to that of the packet itself.

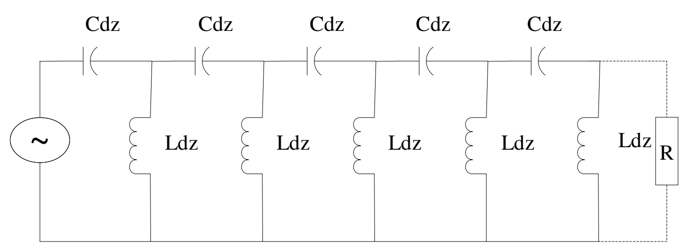

Figure 4.3: Backward wave transmission line $\left(Z = \frac{1}{j\omega C}; Y = \frac{1}{j\omega L}\right)$

4.1.1 Theory

Consider the periodic structure of periodicity p as illustrated in Figure 4.4(b). It consists of series connection of an infinite number of lossless reactive elements at periodic intervals on a uniform waveguide of wave impedance Z_0 and phase constant β_0 for the propagating mode whose unit cells are depicted in Figure 4.4(a). Each unit of the periodic structure can be represented by unit cell ABCD parameters. Such a periodic structure with reactive elements can be equivalently perceived as a new uniform waveguide (wave impedance Z and propagation constant γ) section of length p as illustrated in Figure 4.4(c) and its performance can be modeled in terms of equivalent per-unit-length propagation constant ($\gamma=\alpha+j\beta$) and complex wave impedance (Z=Re(Z)+jIm(Z)). Let us assume that only the dominant mode is propagating. If any other higher order modes are propagating at frequency under consideration then guided-wave parameters for that mode can also be studied in addition to dominant mode. But we will consider guided-wave parameters for the dominant mode only for the sake of simplicity. It is worth mentioning the concept of "accessible" and "localized" modes. Accessible modes are waveguide modes that are being excited at the location of one waveguide discontinuity and are also "seen" by adjacent waveguide discontinuities. This includes all propagating modes of original (unloaded) waveguide, plus, possibly, first few evanescent ones, depending on separation between the two adjacent discontinuities. All remaining modes, purely evanescent, are called localized, as they remain localized to neighborhood of the discontinuity that excites them. The periodicity p of the periodic structures is chosen such that all higher order evanescent modes excited by the waveguide discontinuity have decayed to a negligible value at the next consecutive discontinuities, i.e., all higher order modes are localized. β_0 and Z_0 in Figure 4.4 (a) and Figure 4.4 (b) are respectively the phase constant and wave impedance of dominant mode of the original waveguide (no loading). Whereas, γ and Z are respectively the propagation constant and wave impedance of the corresponding equivalent uniform waveguide of printed periodic waveguide structure (with reactive loading), as illustrated in Figure 4.4(c). If a wave is to propagate down the periodic waveguide structure, it is necessary for voltage and current at the $(n+1)^{th}$ terminal to be equal to voltage and current at the n^{th} terminal, apart from the phase delay due to finite propagation time.

$$\begin{matrix} V_{n+1} = e^{-\gamma p} V_n \\ I_{n+1} = e^{-\gamma p} I_n \end{matrix} \Rightarrow \begin{matrix} V_n = e^{\gamma p} V_{n+1} \\ I_n = e^{\gamma p} I_{n+1} \end{matrix}$$

(4.1)

where $\gamma = \alpha + j\beta$ is propagation constant of the periodic waveguide structure with reactive loading.

In terms of transmission matrix for a unit cell, we now have,

$$\begin{bmatrix} V_n \\ I_n \end{bmatrix} = \begin{bmatrix} A_u & B_u \\ C_u & D_u \end{bmatrix} \begin{bmatrix} V_{n+1} \\ I_{n+1} \end{bmatrix} = e^{\gamma p} \begin{bmatrix} V_{n+1} \\ I_{n+1} \end{bmatrix}$$

$$\Rightarrow \begin{bmatrix} A_u & B_u \\ C_u & D_u \end{bmatrix} - \begin{bmatrix} e^{\gamma p} & 0 \\ 0 & e^{\gamma p} \end{bmatrix} \begin{bmatrix} V_{n+1} \\ I_{n+1} \end{bmatrix} = 0 \quad (4.2)$$

This equation is a matrix eigenvalue equation for γ. Here, the subscript u in ABCD parameters denotes unit/cell.

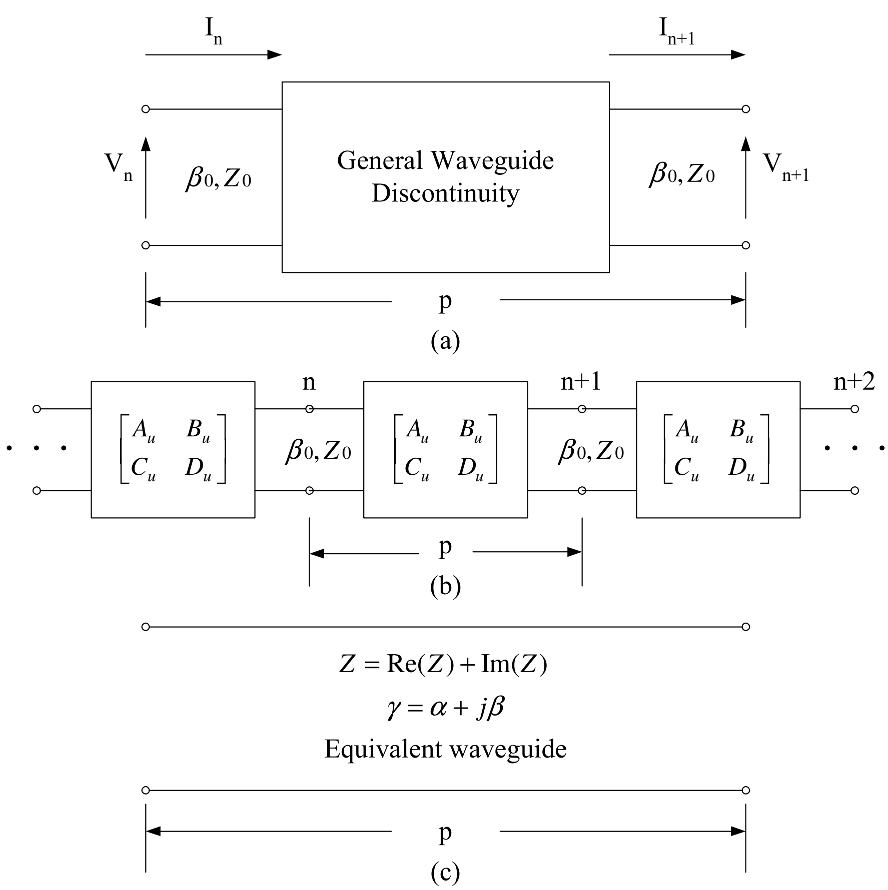

.

Figure 4.4: (a) General waveguide discontinuity as unit/cell for the periodic waveguide structure (b) Infinite periodic waveguide structure composed of cascade connection of units/cells (c) Equivalent uniform waveguide of the infinite periodic waveguide structure

A nontrivial solution for V_{n+1}, I_{n+1} exists only if the determinant vanishes. Hence, considering a reciprocal network in which $A_u D_u - B_u C_u = 1$, we get,

$$\det\left\{\begin{bmatrix} A_u - e^{\gamma p} & B_u \\ C_u & D_u - e^{\gamma p} \end{bmatrix}\right\}$$
$$= A_u D_u - B_u C_u + e^{2\gamma p} - e^{\gamma p}(A_u + D_u)$$
$$= e^{2\gamma p} - e^{\gamma p}(A_u + D_u) + 1 = 0 \qquad (4.3)$$
$$\Rightarrow A_u + D_u = \frac{1 + e^{2\gamma p}}{e^{\gamma p}} = e^{-\gamma p} + e^{\gamma p}$$
$$\Rightarrow \frac{A_u + D_u}{2} = \frac{e^{-\gamma p} + e^{\gamma p}}{2} = \cosh \gamma p$$

So we obtain,

1) Propagation: When $\left|\frac{A_u + D_u}{2}\right| < 1$, we must have $\gamma = j\beta$ and $\alpha = 0$; so that

$$\cos \beta p = \frac{A_u + D_u}{2} \qquad (4.4)$$

2) Attenuation: When $\frac{A_u + D_u}{2} > 1$, we must have $\gamma = \alpha$ and $\beta = 0$; so that

$$\cosh \alpha p = \frac{A_u + D_u}{2} \qquad (4.5)$$

3) Complex mode: When $\frac{A_u + D_u}{2} < -1$, we must have $\gamma p = \alpha + j\pi$, so that

$$\cosh \gamma p = \cosh(\alpha + j\pi) = -\cosh \alpha p = \frac{A_u + D_u}{2} \qquad (4.6)$$

Therefore, depending on the frequency, the periodic structure will exhibit either a passband or stopband. Let us write down the expression for normalized characteristic wave impedance which can be derived similarly for the periodic waveguide structure.

$$\frac{Z}{Z_0} = \frac{V_{n+1}}{I_{n+1}} = \pm\sqrt{\frac{B}{C}} \tag{4.7}$$

The + sign is for forward wave and – sign is for backward wave. Z is real for passband and imaginary for stopband.

Figure 4.5 (b) show the three-dimensional (3-D) geometry of an infinitely extended waveguide based periodic structure loaded with any arbitrary FSS strip and slot layers respectively. The FSS strip/slot layers are transversely put at a periodicity of p inside a uniform waveguide with width of a and height of b. The FSS strips/slots are placed at the symmetrical center of each transverse strip layers inside waveguide. The infinitely extended periodic waveguide structure can be perceived as a 1-D guided-wave medium, thus its per-unit-length medium parameters can be simply analyzed by characterizing a single unit/cell of periodicity p for the periodic waveguide structure. Using the Hybrid MoM-Immittance Approach [1], two-port ABCD parameters of such FSS strip/slot layers driven by two waveguide sections of length p/2 can be numerically derived and hence the guided-wave parameters could be obtained using equations (4.4), (4.5) and (4.7).

4.1.2 Brillouin Diagram

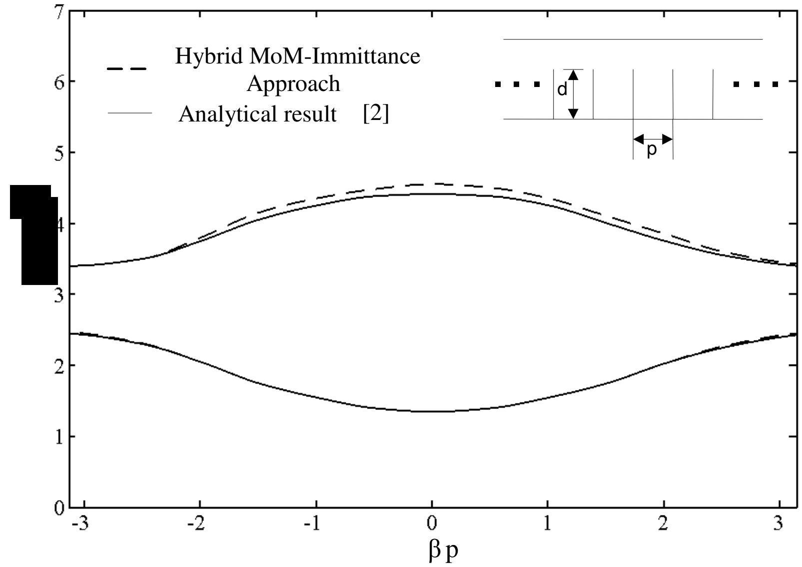
Hybrid MoM-Immittance
Approach
Analytical result [2]
d
p
0
1
2
3
4
5
6
7
-3
-2
-1
0
1
2
3
β p

(a)

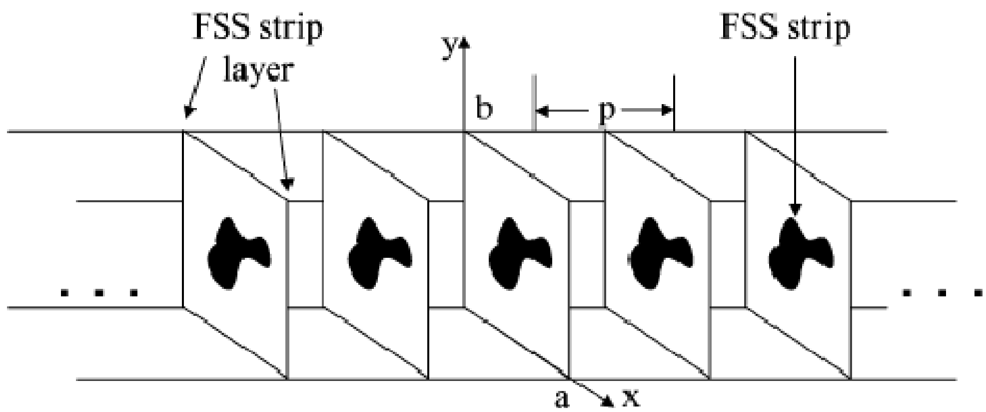
FSS strip
layer
y
b
p
FSS strip
a
x

(b)

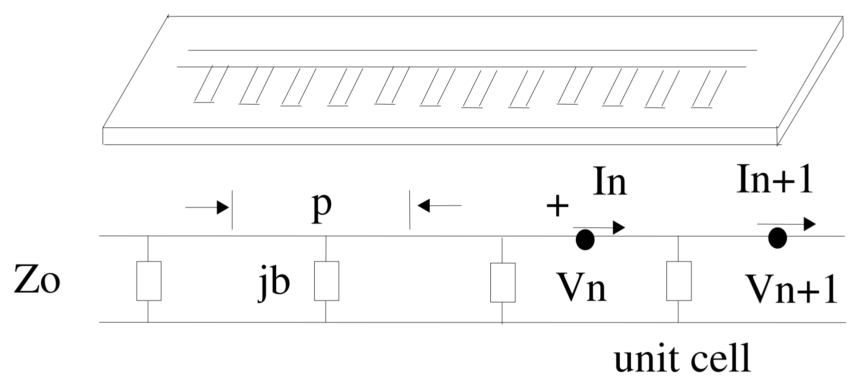
p
+
In
In+1
Zo
jb
Vn
Vn+1
unit cell

(c)

Figure 4.5: (a) Numerically calculated k_0-β diagram for a capacitive strip loaded waveguide based periodic structure (b Periodic waveguide structure loaded with arbitrary FSS structures (c) Microstrip line periodically loaded with a shunt susceptance

A rectangular iris loaded periodic waveguide structure is analyzed. Figure 4.5 (a) shows numerically calculated k_0-β diagram for a rectangular waveguide (22.86mm×5.08mm), loaded with capacitive strips of height d=3.81mm, placed at a period of p=10mm. The Brillouin diagram for the periodic waveguide structure is calculated using the Hybrid MoM-Immittance Approach and compares well with the analytical results given in [2]. From the Brillouin diagram, we can infer the propagation characteristics like slowwave ($\beta/k_0>1$), fastwave ($\beta/k_0<1$), forward wave (v_p and v_g are in the same direction) and backward wave (v_p and v_g are in the opposite direction). From propagation characteristics, we can find the suitable applications of the periodic structures. You may refer to [3], for an indepth study of the waveguide based periodic structures loaded with frequency selective surfaces (FSS). Similar analysis could be carried out for a microstrip line periodically loaded with a shunt susceptance b normalized to the characteristic impedance of the microstrip line.

4.2 Filters

4.2.1 Introduction to filters

Applications of microwave filters can be found in any type of microwave communication, radar, or test and measurement system. A microwave filter is a two-port network used to control the frequency response at a certain point in a microwave system by providing transmission within the passband of the filter and attenuation in the stopband of the filter. At first the image parameter method of filter design was developed in the late 1930s and was useful for low frequency filters in radio and telephony. In these days, most of the microwave filter design is done with sophisticated computer aided design packages based on the insertion loss method. Because of continuing advances in network synthesis with distributed elements, the use of low temperature superconductors, and the incorporation of active devices in filter circuits, microwave filter design remains active research area. Filters designed using the image parameter method consist of a cascade of simpler two-port filter sections to provide the desired cutoff frequencies and attenuation characteristics, but do not allow the specification of a frequency response over the complete operating range. Thus, although the procedure is relatively simple, the design of filters by the image parameter method often must be iterated many times to achieve the desired results. A more modern procedure, called the insertion loss method, uses network synthesis techniques to design filters with completely specified frequency response. The design is simplified by beginning with low-pass filter prototypes that are normalized in terms of impedance and frequency. Transformations are then applied to convert the prototype designs to the desired frequency range and impedance level. Both the image parameter and insertion loss method of filter design provide lumped element circuits. For microwave applications such designs usually must be modified to use distributed elements consisting of transmission line sections.

Filter parameter definition

Some very important specifications for the design of filters are frequency range, bandwidth, insertion loss, stopband attenuation and frequencies, input and output impedance levels, voltage standing-wave ratio (VSWR), group delay, phase linearity, temperature range, and transient response. The input of a filter is driven by a signal generator with the output passing to a load. At the input plane of the filter, the power may be broken into three components;

P_{in}, the incident power from the generator;

P_R, the power reflected back to the generator;

P_A, the power absorbed by the filter;

and P_L, the power passed on to the load.

Insertion Loss

The insertion loss IL (in decibels) at a particular frequency is defined as

$$IL = 10 \log (P_{LR}) = 10 \log (P_{in} / P_L) = -10 \log \left(|\tau|^2 \right) = -10 \log \left(|S_{21}|^2 \right)$$

Return Loss

Three related parameters, the return loss (RL), VSWR, and reflection coefficient (ρ), are commonly used to characterize filter reflections. Return loss is used with filters because it is a sensitive parameter describing filter performance. The return loss is the ratio to input to reflected power.

$$RL = -10 \log (P_R / P_{in})$$

$$= -10 \log \left(\frac{\text{VSWR} - 1}{\text{VSWR} + 1} \right)^2$$

$$= -10 \log \left(|\Gamma|^2 \right) = -10 \log \left(|S_{11}|^2 \right)$$

Basic types of filters and applications

Basically there are four types of filters: low pass, high pass, band pass and band stop (also called band reject or notch). An ideal filter would have zero insertion loss and constant group delay across the desired frequency passbands and infinite rejection everywhere else. All filters exhibit spurious responses where they have rejection in the passband or regions of low loss where the rejection should be high. The best that can be accomplished is to have the filter perform well over frequencies of interest. Over the past decade, the explosive growth in wireless communication and other portable receiver and transmitter applications has generated a significant market for low loss, smaller size, light weight, and low cost filters. Various technologies such as ceramic block, low-temperature co-fired ceramic (LTCC), micromachining, and high-temperature superconductors are being pursued to meet often stringent requirements for RF filters. Almost all microwave receivers, transmitters, and test setups require filter action, the main filter functions are to reject undesirable signal frequencies outside the filter passband and to channelize or combine different frequency signals. Good examples for the former applications are mixers (low pass) and multipliers (band pass). A well described example for the latter application is the channelized receiver in which a bank of filters is used to separate input signals. Specific applications include electronic support measure (ESM) receivers, satellite communications, mobile communications, direct broadcast satellite systems, pulse code modulation (PCM) communications, and microwave FM multiplexers.

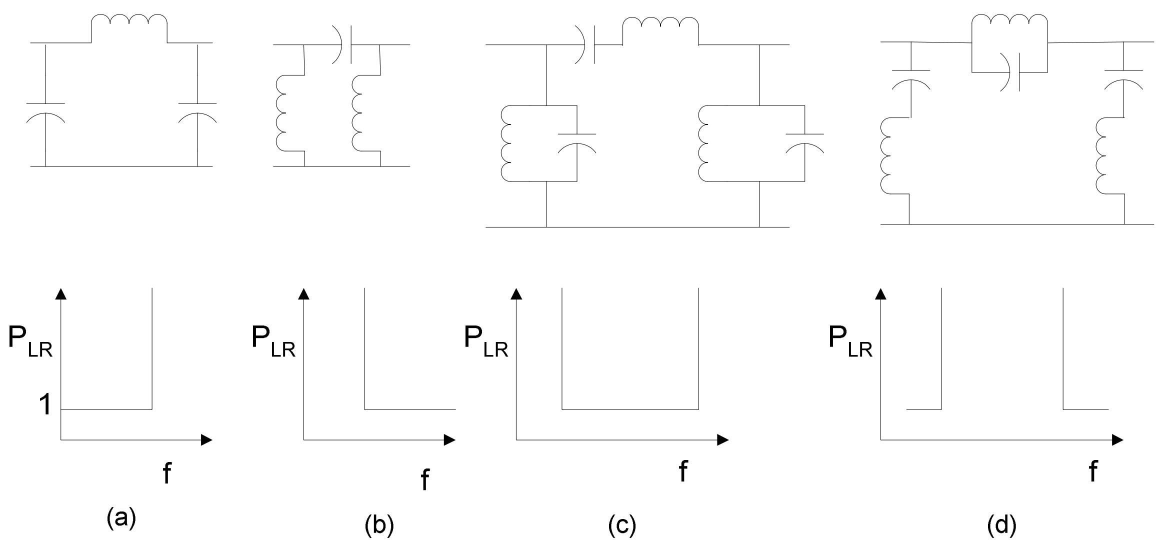

Fig. 4.6 Lump element network representations and filter characteristics of various filters (a) low pass (b) high pass (c) band pass and (d) band stop

4.2.2 Filter synthesis

Several methods are available for designing filters. Of these, the low pass prototype filter synthesis and numerical method have been the most successful. Despite drawbacks, the traditional technique (low pass prototype) has been very successful and has been the basis for the vast majority of filter designs. The traditional design is the starting point for the second type of design using numerical methods.

Filter design from low pass filter synthesis

This method consists of the following steps:

1. Design of a prototype low pass filter with the desired passband characteristics,
2. Transformation of this prototype network to the required type (low pass, high pass, band pass or band stop) filter with the specified center and/or band-edge frequencies, and
3. Realization of the network in terms of lumped and/or distributed circuit elements.

Low pass prototype filter design using the insertion loss method is used extensively. In this method the design of the filter starts with specifying the insertion loss and the return loss for a lossless network over the desired frequency band. The combination of inductors and capacitors shown in Fig. below is obviously a low pass circuit. There are many numbers of ways to choose the element values for a low pass prototype design. The two most widely used solutions are the maximally flat (Butterworth) response, and equal ripple (Chebyshev also often spelled Tchebycheff)

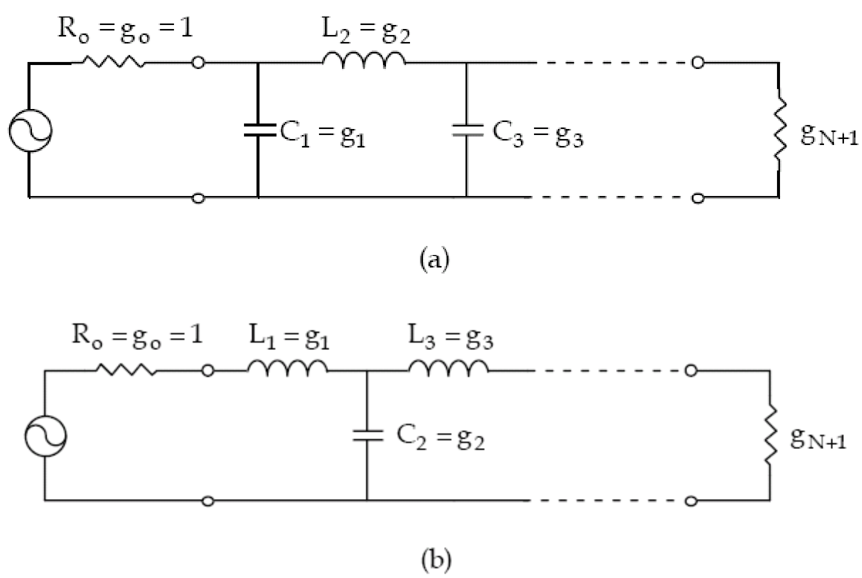

Fig. 4.7 Lumped element network of low pass prototype filter

The transfer function for a two-port filter network is a mathematical description of network response characteristics, specifically the transmission coefficient S_{21}. On many occasions, an amplitude squared transfer function for a low loss passive filter network is defined as

$$\left| S_{21}(j\Omega) \right|^2 = \frac{1}{1+\varepsilon^2 F_n^2(\Omega)}$$

where ε is a ripple constant, F_n (Ω) represents a filtering or characteristic function and Ω is a frequency variable (also represented by $\frac{\omega}{\omega_c}$). In a low pass filter prototype filter Ω represents the radian frequency where $\Omega = \Omega_c$ is the cutoff frequency for $\Omega_c = 1$ (rad / s). The transfer functions for Butterworth (ε=1 for this case) and Chebyshev responses respectively are

$$\left| S_{21}(j\Omega) \right|^2 = \frac{1}{1+\Omega^{2n}}$$

$$\left| S_{21}(j\Omega) \right|^2 = \frac{1}{1+\varepsilon^2 T_n^2(\Omega)}$$

where the ripple constant ε is related to a given passband ripple L_{Ar} in dB by

$$\varepsilon = \sqrt{10^{\frac{L_{Ar}}{10}} - 1}$$

T_n (Ω) is a Chebyshev function of the first kind of order n, which is defined as

$$T_n(\Omega) = \begin{cases} \cos\left(n\cos^{-1}\Omega \right) & |\Omega| \le 1 \\ \cosh\left(n\cosh^{-1}\Omega \right) & |\Omega| \ge 1 \end{cases}$$

The element values of the Butterworth and Chebyshev responses are obtained respectively by using the formulae listed below.

Butterworth response:

$$g_0 = 1.0$$

$$g_i = 2\sin\left(\frac{(2i-1)\pi}{2n} \right) \qquad \text{for } i = 1 \text{ to } n$$

$$g_{n+1} = 1.0$$

To determine the degree of a Butterworth low pass prototype, a specification that is usually the minimum stopband attenuation L_{As} dB at $\Omega = \Omega_s$ for $\Omega_s > 1$ is given. Hence

$$n \geq \frac{\log\left(10^{0.1L_{As}} - 1\right)}{2\log\Omega_s}$$

$$\because IL = L_{As} = 20\log\left(\left|S_{21}\right|\right) = 10\times\log\left(1+\Omega_s^{2n}\right) \Rightarrow 10^{\frac{L_{As}}{10}} - 1 = \Omega_s^{2n} \Rightarrow n = \frac{\log\left(10^{\frac{L_{As}}{10}} - 1\right)}{2\log\Omega_s}$$

Chebyshev response:

$$g_0 = 1.0$$

$$g_1 = \frac{2}{\gamma}\sin\left(\frac{\pi}{2n}\right)$$

$$g_i = \frac{1}{g_{i-1}} \frac{4\sin\left(\frac{(2i-1)\pi}{2n}\right)\sin\left(\frac{(2i-3)\pi}{2n}\right)}{\gamma^2 + \sin^2\left(\frac{(i-1)\pi}{n}\right)}$$

$$g_{n+1} = \begin{cases} 1.0 & \text{for n odd} \\ \coth^2\left(\frac{\beta}{4}\right) & \text{for n even} \end{cases}$$

where

$$\beta = \ln\left[\coth\left(\frac{L_{Ar}}{17.37}\right)\right]$$

$$\gamma = \sinh\left(\frac{\beta}{2n}\right)$$

and g_0, g_1, …..,g_{n+1} are element values.

For the required passband ripple L_{Ar} dB, the minimum stopband attenuation L_{As} dB at $\Omega = \Omega_s$ for $\Omega_s > 1$, the degree of Chebyshev low pass prototype is given by

$$n \geq \frac{\cosh^{-1}\left(\sqrt{\frac{10^{01L_{As}}-1}{10^{01L_{Ar}}-1}}\right)}{\cosh^{-1}(\Omega_s)}$$

$$\because IL = L_{As} = 20\log\left(|S_{21}|\right) = 10\times\log\left(1+\varepsilon^2 T_n^2\right)$$

$$\Rightarrow \frac{10^{\frac{L_{As}}{10}}-1}{\varepsilon^2} = \frac{10^{\frac{L_{As}}{10}}-1}{10^{\frac{L_{Ar}}{10}}-1} = T_n^2 = \left(\cosh n \cosh^{-1}\Omega_s\right)^2 \Rightarrow n = \frac{\cosh^{-1}\sqrt{\frac{10^{\frac{L_{As}}{10}}-1}{10^{\frac{L_{Ar}}{10}}-1}}}{\cosh^{-1}\Omega_s}$$

After the filter order was determined the element values have been computed for respective filter realizations.

Impedance and Frequency transformations

The low pass prototype filers realized with normalized resistance/conductance and cutoff frequencies have to be transformed to the actual filter type at the cutoff frequencies. The frequency transformation, which is also referred to as the frequency mapping is required to map a response such as Chebyshev response in the low pass prototype frequency domain $\Omega = \frac{\omega}{\omega_c}$ to that in the frequency domain ω in which a practical filter response such as low pass, high pass, band pass and band stop are expressed. The frequency transformation shows effect on reactive elements accordingly but no effect on the resistive elements. In addition to the frequency mapping, impedance scaling is also required to accomplish the element transformation. The impedance scaling will remove the g_0 = 1 normalization and adjust the filter to work for any value of source impedance denoted by R_0. In principle, applying the impedance scaling upon a filter network in such a way that

$$L' \rightarrow R_0 L$$

$$C' \rightarrow C/R_0$$

$$R' \rightarrow R_0 R$$

$$G' \rightarrow G/R_0$$

has no effect on the response shape.

Let g be the generic term for low pass prototype elements in the element transformation to be discussed. Because it is independent of the frequency transformation, the following resistive element transformation holds for any type of filter.

$$R' = R_0 g \qquad \text{for g representing the resistance}$$

$$G' = \frac{g}{R_0} \qquad \text{for g representing the conductance}$$

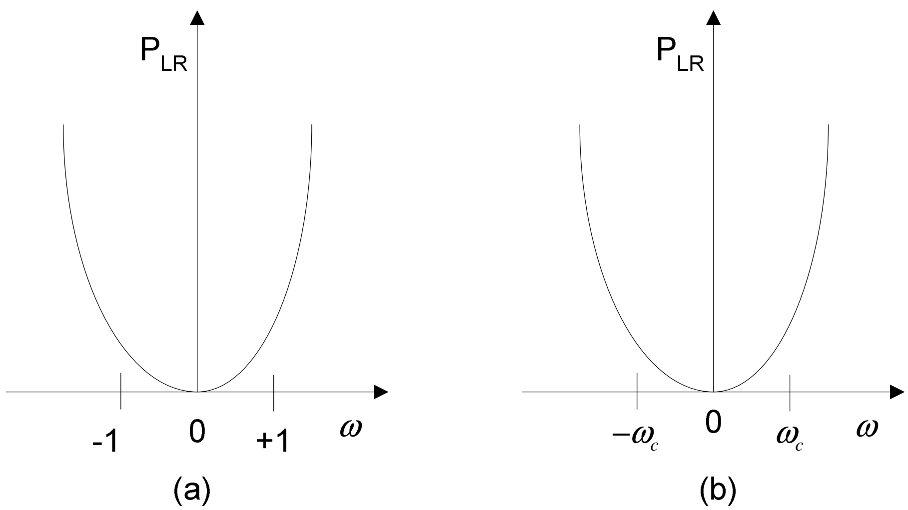

Fig. 4.8 (a) Low pass filter prototype response (b) Frequency transformation for low pass filter

Low pass transformation

The frequency transformation from a low pass prototype to a practical filter having cutoff frequency ω_c in the angular frequency axis ω is simply given by the following relations.

After frequency transformation

$$\because 1 \to \omega_c \Rightarrow \frac{\omega}{\omega_c} \to \omega$$

$$P'_{LR}(\omega) = P_{LR}(\frac{\omega}{\omega_c})$$

$$\Rightarrow jX_L = j\frac{\omega}{\omega_c}L = j\omega L' \Rightarrow L' = \frac{L}{\omega_c}$$

$$\Rightarrow jB_c = j\frac{\omega}{\omega_c}C = j\omega C' \Rightarrow C' = \frac{C}{\omega_c}$$

After doing impedance transformation as well

$$L^{'} = \frac{LR_0}{\omega_c}; C^{'} = \frac{C}{\omega_c R_0}$$

High pass transformation

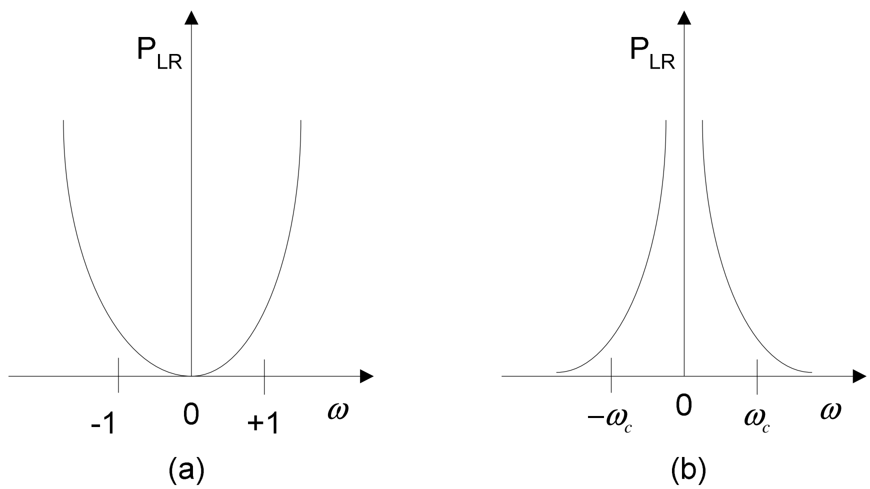

Fig. 4.9 (a) Low pass filter prototype response (b) Frequency transformation for high pass filter

For high pass filters with cutoff frequency ω_c in the ω –axis, the frequency transformation is as follows.

After frequency transformation

$$\because 0 \rightarrow \pm\infty, 1 \rightarrow -\omega_c, -1 \rightarrow \omega_c \Rightarrow -\frac{\omega_c}{\omega} \rightarrow \omega$$

$$P_{LR}^{'}(\omega) = P_{LR}(-\frac{\omega_c}{\omega})$$

$$\Rightarrow jX_L = -j\frac{\omega_c}{\omega}L = \frac{1}{j\omega C^{'}} \Rightarrow C^{'} = \frac{1}{\omega_c L}$$

$$\Rightarrow jB_c = -j\frac{\omega_c}{\omega}C = \frac{1}{j\omega L^{'}} \Rightarrow L^{'} = \frac{1}{\omega_c C}$$

After doing impedance transformation as well

$$L^{'} = \frac{R_0}{\omega_c C}; C^{'} = \frac{R_0}{\omega_c L}$$

Note that after frequency transformation, inductor in the low pass filter prototype will become capacitor and vice versa.

Band pass transformation

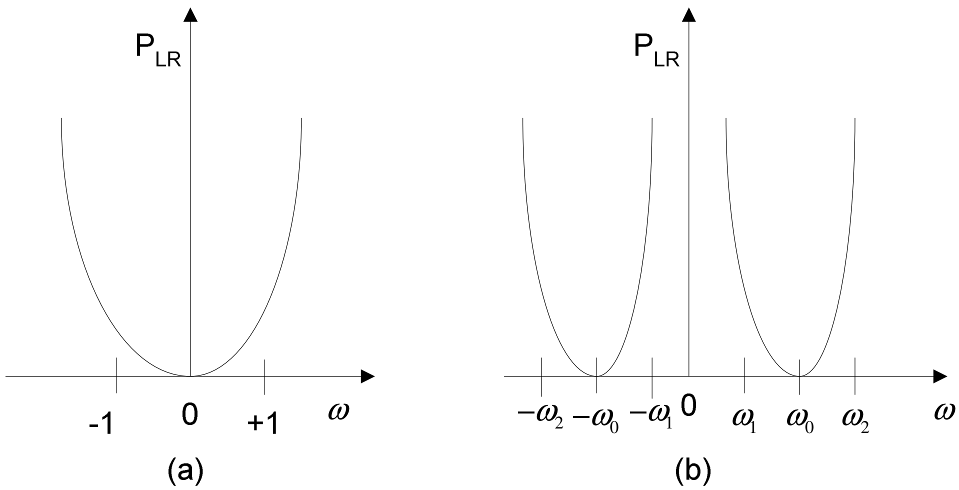

Fig. 4.10 (a) Low pass filter prototype response (b) Frequency transformation for band pass filter

The frequency transformation from low pass prototype response to band pass response having a passband ω_2-ω_1, where ω_1 and ω_2 indicate the passband edge angular frequency is given as below.

$$\because 0 \rightarrow \omega_0, 1 \rightarrow \omega_2, -1 \rightarrow \omega_1 \Rightarrow \frac{1}{\Delta}\left(\frac{\omega}{\omega_0} - \frac{\omega_0}{\omega}\right) \rightarrow \omega, \omega_0 = \sqrt{\omega_1 \omega_2}, \Delta = \frac{\omega_2 - \omega_1}{\omega_0}$$

$$P_{LR}^{'}(\omega) = P_{LR}\left(\frac{1}{\Delta}\left(\frac{\omega}{\omega_0} - \frac{\omega_0}{\omega}\right)\right)$$

$$\Rightarrow jX_L = j\frac{1}{\Delta}\left(\frac{\omega}{\omega_0} - \frac{\omega_0}{\omega}\right)L = j\omega L^{'} + \frac{1}{j\omega C^{'}} \Rightarrow L^{'} = \frac{L}{\omega_0 \Delta}, C^{'} = \frac{\Delta}{\omega_0 L}$$

$$\Rightarrow jB_c = j\frac{1}{\Delta}\left(\frac{\omega}{\omega_0} - \frac{\omega_0}{\omega}\right)C = j\omega C^{'} + \frac{1}{j\omega L^{'}} \Rightarrow C^{'} = \frac{C}{\omega_c \Delta}, L^{'} = \frac{\Delta}{\omega_c C}$$

Note that inductor in the low pass filter prototype will give series LC circuit and capacitor in the low pass filter prototype will give shunt LC circuit after the frequency transformation.

Band stop transformation

The frequency transformation from low pass prototype to band stop is achieved by the frequency mapping.

$$\because 0 \to \pm\infty, 1 \to \omega_1, -1 \to \omega_2 \Rightarrow \frac{\Delta}{(\frac{\omega_0}{\omega} - \frac{\omega}{\omega_0})} \to \omega, \omega_0 = \sqrt{\omega_1\omega_2}, \Delta = \frac{\omega_2 - \omega_1}{\omega_0}$$

$$P_{LR}^{'}(\omega) = P_{LR}(\frac{\Delta}{(\frac{\omega_0}{\omega} - \frac{\omega}{\omega_0})})$$

$$\Rightarrow jX_L = j\frac{\Delta}{(\frac{\omega_0}{\omega} - \frac{\omega}{\omega_0})}L = \frac{1}{(\frac{\omega_0}{j\Delta L\omega} + j\frac{\omega}{\Delta L\omega_0})} = \frac{1}{\frac{1}{j\omega L^{'}} + j\omega C^{'}} \Rightarrow L^{'} = \frac{L\Delta}{\omega_0}, C^{'} = \frac{1}{\Delta\omega_0 L}$$

$$\Rightarrow jB_c = j\frac{\Delta}{(\frac{\omega_0}{\omega} - \frac{\omega}{\omega_0})}C = \frac{1}{(\frac{\omega_0}{j\Delta C\omega} + \frac{j\omega}{\Delta C\omega_0})} = \frac{1}{\frac{1}{j\omega L^{'}} + j\omega C^{'}} \Rightarrow L^{'} = \frac{\Delta C}{\omega_0}, C^{'} = \frac{1}{\omega_0\Delta C}$$

Note that inductor in the low pass filter prototype becomes shunt LC resonator circuit and capacitor in the low pass filter prototype becomes series LC resonator circuit after band stop filter transformation.

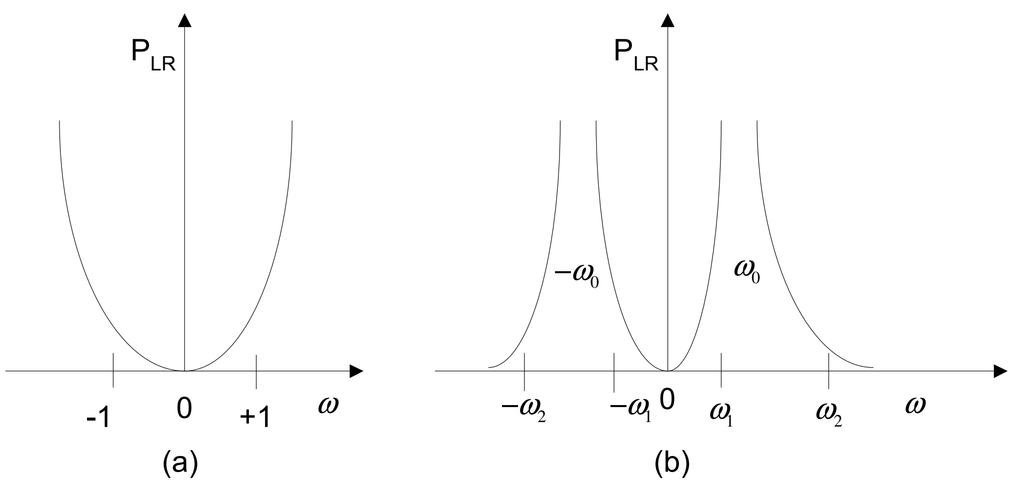

Fig.4.11 (a) Low pass filter prototype response (b) Frequency transformation for band stop filter

After frequency transformations, impedance scaling could be done by multiplying all the inductors by R_0 and dividing all the capacitors by R_0.

Example 4.1

Design a maximally flat low pass filter with a cut-off frequency of 2GHz, impedance 50 ohm and at least 15dB insertion loss at 3GHz.

Solution:

$$n \geq \frac{\log\left(10^{0.1L_{As}} - 1\right)}{2\log\frac{\omega_s}{\omega_c}} = \frac{\log\left(10^{0.1\times15} - 1\right)}{2\log\left(\frac{3}{2}\right)} = 4.2 \text{ choose n=5}$$

Prototype elements:

$$g_0 = 1.0$$

$$g_1 = 2\sin\left(\frac{(2\times 1-1)\pi}{2\times 5}\right) = 0.618$$

$$g_2 = 2\sin\left(\frac{(2\times 2-1)\pi}{2\times 5}\right) = 1.618$$

$$g_3 = 2\sin\left(\frac{(2\times 3-1)\pi}{2\times 5}\right) = 2.00$$

$$g_4 = 2\sin\left(\frac{(2\times 4-1)\pi}{2\times 5}\right) = 1.618$$

$$g_5 = 2\sin\left(\frac{(2\times 5-1)\pi}{2\times 5}\right) = 0.618$$

$$g_6 = 1.0$$

$$C_1^{'} = \frac{C_1}{R_0\omega_c} = 0.983\,pF$$

$$L_2^{'} = \frac{L_2R_0}{\omega_c} = 6.438\,nH$$

$$C_3^{'} = \frac{C_3}{R_0\omega_c} = 3.183\,pF$$

$$L_4^{'} = \frac{L_4R_0}{\omega_c} = 6.438\,nH$$

$$C_5^{'} = \frac{C_5}{R_0\omega_c} = 0.983\,pF$$

$$R_s^{'} = g_0R_0 = 50\Omega;\ R_L^{'} = g_6R_0 = 50\Omega$$

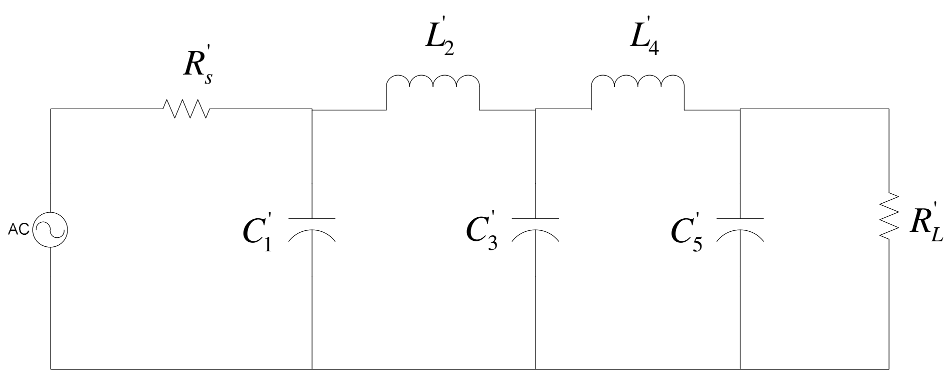

Fig. 4.12 Low Pass Filter LC equivalent circuit for Example 4.1

Example 4.2

Design a 3rd order 0.5dB equi-ripple band pass filter at a center frequency of 1GHz, impedance 50 ohm and BW of 10%.

Solution:

$$g_0 = 1.0$$

$$\beta = \ln\left[\coth\left(\frac{0.5}{17.37}\right)\right] = 3.548$$

$$\gamma = \sinh\left(\frac{\beta}{2n}\right) = \sinh\left(\frac{3.548}{2\times 3}\right) = 0.626$$

$$g_1 = \frac{2}{\gamma}\sin\left(\frac{\pi}{2n}\right) = \frac{2}{0.626}\sin\left(\frac{\pi}{2\times 3}\right) = 1.597$$

$$g_2 = \frac{1}{1.597}\frac{4\sin\left(\frac{(2\times 2-1)\pi}{2\times 3}\right)\sin\left(\frac{(2\times 2-3)\pi}{2\times 3}\right)}{0.626^2+\sin^2\left(\frac{(2-1)\pi}{3}\right)} = 1.0967$$

$$g_3 = \frac{1}{1.0967}\frac{4\sin\left(\frac{(2\times 3-1)\pi}{2\times 3}\right)\sin\left(\frac{(2\times 3-3)\pi}{2\times 3}\right)}{0.626^2+\sin^2\left(\frac{(3-1)\pi}{3}\right)} = 1.597$$

$$g_4 = 1$$

$$L_1^{'} = \frac{L_1 R_0}{\omega_0 \Delta} = 127.0nH \quad C_1^{'} = \frac{\Delta}{\omega_0 L_1 R_0} = 0.199\,pF$$

$$L_2^{'} = \frac{\Delta R_0}{\omega_0 C_2} = 0.726nH \quad C_2^{'} = \frac{C_2}{\omega_0 \Delta R_0} = 34.91\,pF$$

$$L_3^{'} = \frac{L_3 R_0}{\omega_0 \Delta} = 127.0nH \quad C_3^{'} = \frac{\Delta}{\omega_0 L_3 R_0} = 0.199\,pF$$

$$R_s^{'} = g_0 R_0 = 50\Omega; R_L^{'} = g_4 R_0 = 50\Omega$$

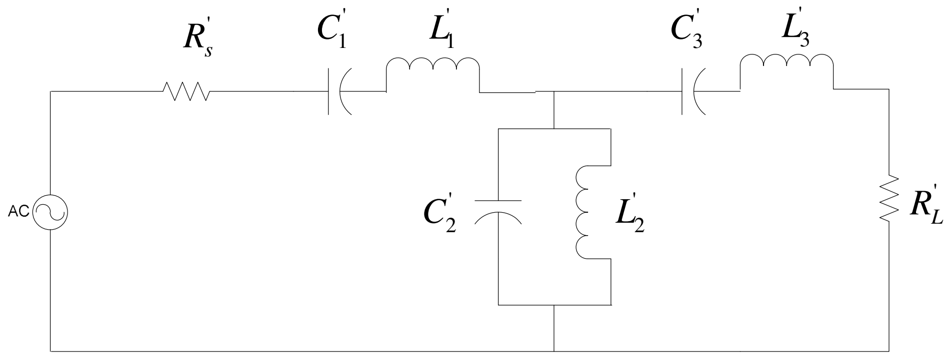

Fig. 4.13 Band Pass Filter Equivalent Circuit for Example 4.2

4.2.3 Practical Filter Examples

Stepped Impedance Low Pass Filter

A popular low pass filter is stepped impedance or hi-Z and low-Z filter, it takes up less space than low pass filter using stubs. Consider a transmission line with characteristic impedance of Z_0 and length 'l'.

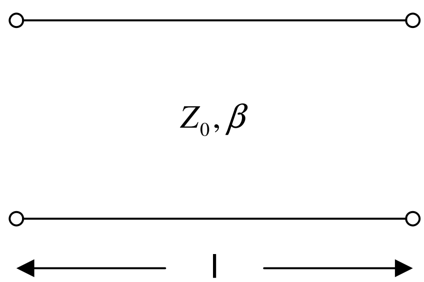

Fig. 4.14 A transmission line of length l

It can be expressed as a 2-port microwave network and described in terms of impedance parameters as $V_1 = Z_{11} I_1 + Z_{12} I_2$ and $V_2 = Z_{21} I_1 + Z_{22} I_2$.

The [ABCD] matrix of a transmission line of length l can be expressed as

$$\begin{pmatrix} A & B \\ C & D \end{pmatrix} = \begin{pmatrix} \cos\beta l & jZ_0 \sin\beta l \\ jY_0 \sin\beta l & \cos\beta l \end{pmatrix}$$

Now values of elements of [Z] matrix can be obtained from the [ABCD] matrix of a transmission line as follows

$$\begin{pmatrix} Z_{11} & Z_{12} \\ Z_{21} & Z_{22} \end{pmatrix} = \frac{1}{C}\begin{pmatrix} A & AD-BC \\ 1 & D \end{pmatrix}$$

For a reciprocal network $AD-BC$, therefore,

$$\begin{pmatrix} Z_{11} & Z_{12} \\ Z_{21} & Z_{22} \end{pmatrix} = \frac{1}{C}\begin{pmatrix} A & 1 \\ 1 & D \end{pmatrix}$$

Hence, $Z_{11} = Z_{22} = A/C = -jZ_0 \cot(\beta l)$ and $Z_{12} = Z_{21} = 1/C = -jZ_0 \text{cosec}(\beta l)$. Since a small section of transmission line is a reciprocal network and hence it can be represented by T-equivalent circuit as follows:

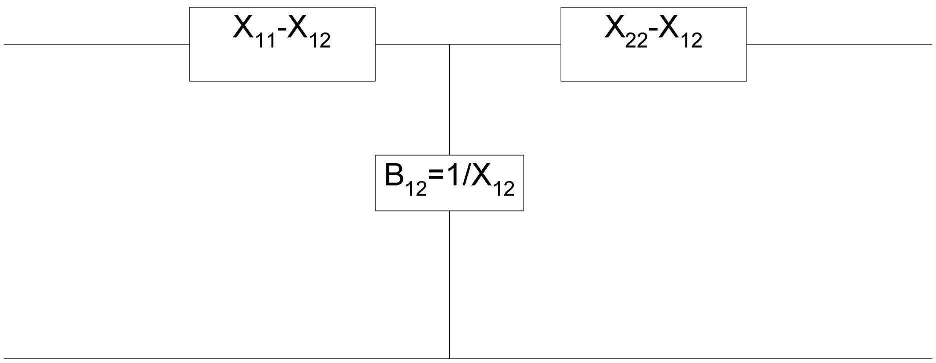

Fig. 4.15 Two-port T-equivalent network

Then series element is $Z_{11} - Z_{22} = -jZ_0[(\cos(\beta l)-1)/\sin(\beta l)] = j Z_0 \tan(\beta l/2)$ and the shunt element is simply $Z_{12} = -jZ_0 \text{cosec}(\beta l)$. So, if $\beta l < \pi/2$, the series elements have a positive reactance (inductors), while the shunt element has a negative reactance i.e. a capacitor.

$X/2 = Z_0 \tan(\beta l/2)$,

$B = \sin(\beta l)/ Z_0$,

For a short line say $\beta l < \pi/4$ and a large characteristic impedance we get,

$X \approx Z_0 \beta l$,

$B \approx 0$,

and a small characteristic impedance we get,

$X \approx 0$,

$B \approx \beta l/ Z_0$,

which implies that large characteristic impedance ($Z_0 = Z_h$) results in series inductor while small characteristic impedance ($Z_0 = Z_l$) result in shunt capacitor.

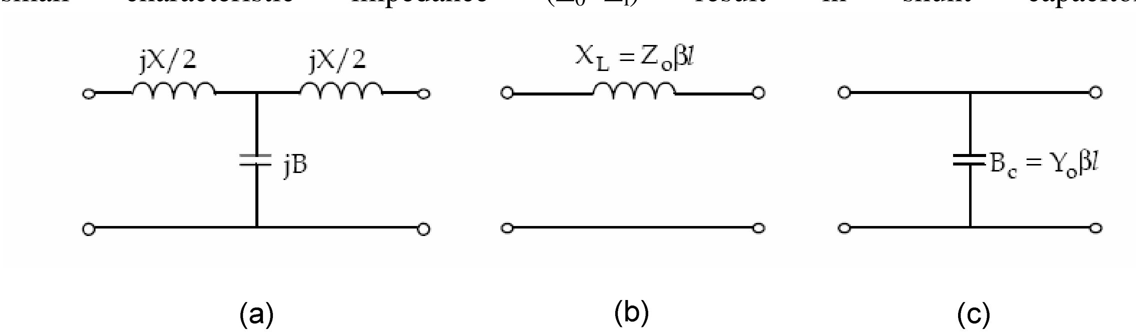

Fig. 4.16 Equivalent circuit of a transmission line of length of l (a) General case (b) For large Z_0 and (c) For small Z_0

And the electrical lengths of the individual sections can be calculated at $\omega_c = 1$ (normalized frequency) as,

$$X = \omega_c L' = \omega_c \frac{L}{\omega_c} R_0 = LR_0 \cong Z_h \beta l \Rightarrow \beta l = \frac{LR_0}{Z_h} \text{ (inductor)},$$

$$B = \omega_c C' = \omega_c \frac{C}{\omega_c R_0} = \frac{C}{R_0} \cong \frac{\beta l}{Z_l} \Rightarrow \beta l = \frac{Z_l C}{R_0} \text{ (capacitor)},$$

where R_0 is the filter impedance and L and C are the normalized element values (g_ks) of the low pass prototype.

Example 4.3

Let us design a low-pass filter with f_c =1.5GHz, maximally flat response in pass band and attenuation in stopband should be > 20 dB at 2.25GHz. Assume low impedance is 50ohm, high impedance is 100 ohm and filter impedance is 50 ohm. Use FR4 substrate.

Solution:

Filter specifications:

Cutoff frequency (f_c) = 1.5GHz

IL of 20dB at 2.25GHz frequency

Board Specifications:

FR4 board

Substrate's dielectric constant (ε_r) = 4.4

Substrate's thickness (d) = 1.6 mm

Taking Z_h = 100 Ω and Z_l = 20 Ω and R_0 = 50 Ω, the widths and effective dielectric constants can be found as

$W/d = 8e^A/(e^{2A}-2)$ for W/d <2

$= 2[B-1-\ln(2B-1)+ (\varepsilon_r -1)\{\ln(B-1)+0.39-0.61/ \varepsilon_r \}/2 \varepsilon_r]/\pi$ for W/d>2

$A = Z_0 \text{sqrt}((\varepsilon_r+1)/2) + (\varepsilon_r-1)/ (\varepsilon_r+1)(0.23+0.11/ \varepsilon_r)$

$B = 377 \pi / (2 Z_0 \text{sqrt}(\varepsilon_r))$

where Z_0 is the characteristic impedance of the section and

$\varepsilon_e = (\varepsilon_r+1)/2 + (\varepsilon_r-1)/2\text{sqrt}(1+12d/W)$

For a capacitive section i.e. Z_l = 20 Ω

W = 11.1057 mm

ε_e = 3.7291

For an inductive section i.e. Z_h = 100 Ω

W = 0.7092 mm

ε_e = 3.020

For resistive section i.e. Z_0 = 50 Ω

W= 3.05mm

For a maximally flat low pass filter, the order of the filter is

$$n \geq \frac{\log\left(10^{0.1L_{As}}-1\right)}{2\log\Omega_s} = \frac{\log\left(10^{0.1\times 20}-1\right)}{2\log\frac{2.25}{1.5}} = 5.67$$

So order of filter is taken to be 6. We can calculate these values using formula $g_i = 2\sin\left(\frac{(2i-1)\pi}{2n}\right)$ where n is the order of filter. And from the g_i values following parameters of the filter are be obtained and tabularized below:

g_i	βl_i (rad)	βl_i (deg)	W_i (mm)	l_i (mm)

1	0.517	0.2068	11.8488	11.1057	3.4088
2	1.414	0.7070	40.5081	0.7092	12.9481
3	1.932	0.7728	44.2782	11.1057	12.7384
4	1.932	0.9660	55.3477	0.7092	17.6915
5	1.414	0.5656	32.4065	11.1057	9.3230
6	0.517	0.2585	14.8110	0.7092	4.7342

Table 4.1

g_7=1, which means the filter is terminated by a section of transmission line with characteristic impedance of 50Ω and length of this line is taken to be 7 mm. Note that for calculation of li for various parts of the stepped impedance low pass filter, we will use the formula for calculation of $\beta = \frac{2\pi}{\lambda_g} = \frac{2\pi\sqrt{\varepsilon_e}}{\lambda}$. The value of effective ε is also dependent on the width of the microstrip line. Since there are two different widths of the microstrip line for this filter depending on the value of Z_{low} and Z_{high}, we will have two different values of β. We have simulated this stepped impedance low pass filter using full-wave simulation software High Frequency Structure Simulator (HFSS) and we observe that the LPF has cut-off frequency at 1.5GHz and insertion loss level at 2.25GHz is around 20dB.

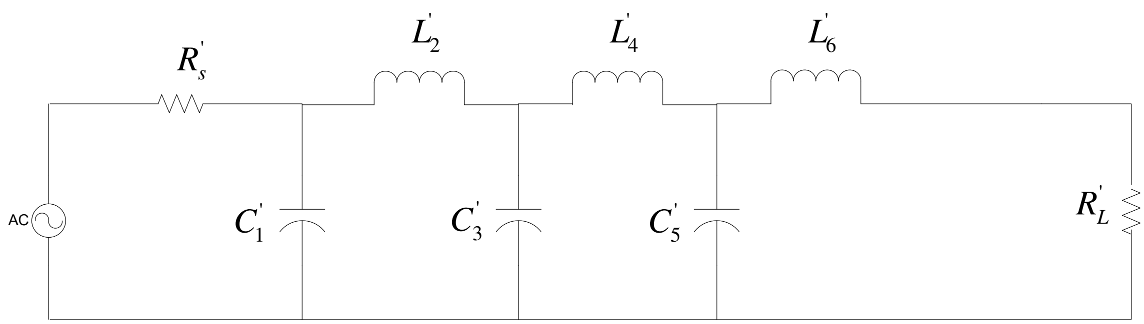

(a)

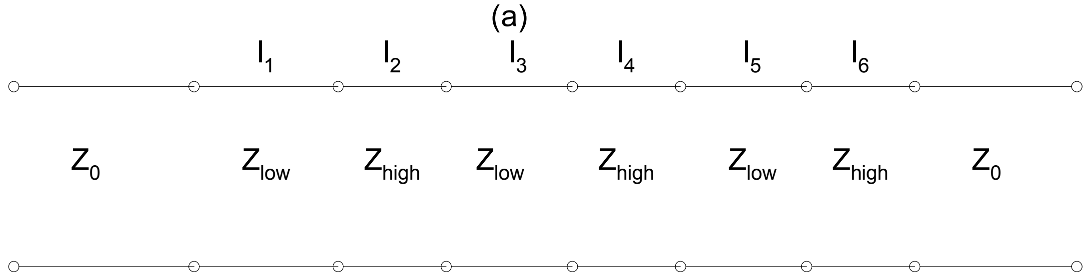

(b)

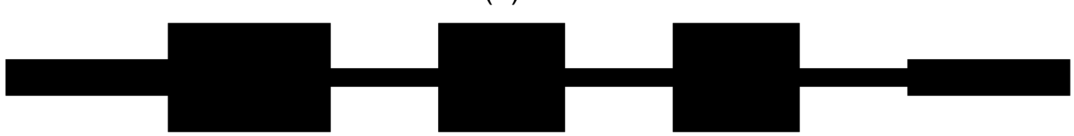

(c)

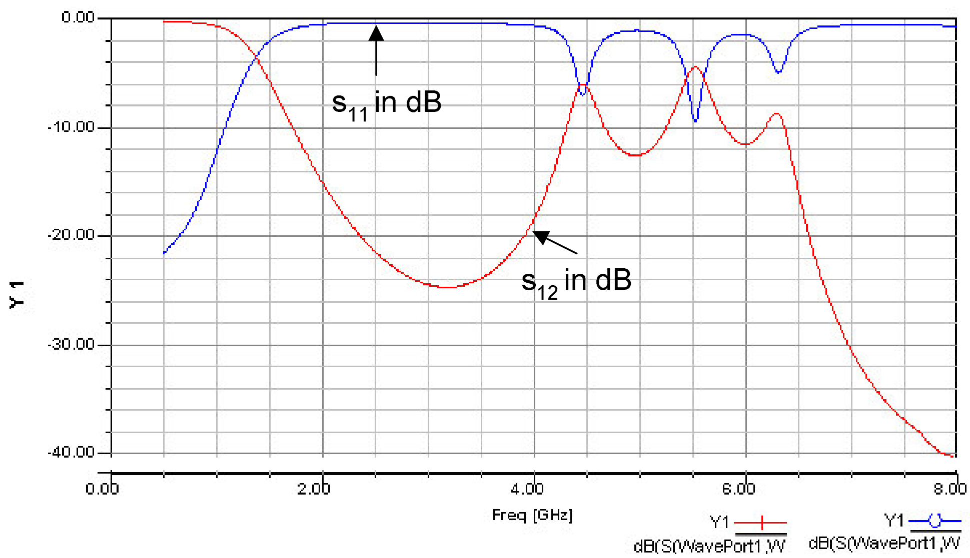

(d)

Fig. 4.17 (a) 6th order low pass filter prototype (b) Stepped impedance implementation (c) Microstrip layout of the filter (d) Scattering parameters of the Stepped-impedance LPF

Parallel Coupled Half-wavelength resonator filters (not included in syllabus)

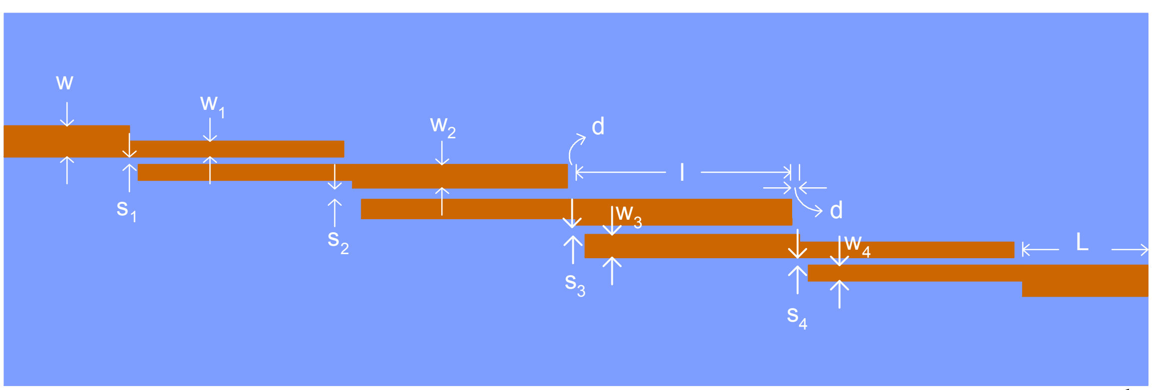

Fig. 4.18 Parallel Coupled Half-wavelength resonator filters showing its dimensions (3rd order)

Fig. 4.18 illustrates a general structure of parallel coupled microstrip band pass filters that use half wavelength line resonators. They are positioned so that adjacent resonators are parallel to each other along half of their length. This parallel arrangement gives relatively large coupling for a given spacing between resonators, and thus, this filter structure is particularly convenient for constructing filters having a wider bandwidth. The design equations for this filter are given by

$$\frac{J_{0,1}}{Y_0} = \sqrt{\frac{\pi}{2}\frac{FBW}{g_0 g_1}}$$

$$\frac{J_{j,j+1}}{Y_0} = \frac{\pi FBW}{2}\frac{1}{\sqrt{g_j g_{j+1}}} \qquad j = 1 \text{ to } n\text{-}1$$

$$\frac{J_{n,n+1}}{Y_0} = \sqrt{\frac{\pi}{2}\frac{FBW}{g_n g_{n+1}}}$$

where $J_{j,j+1}$ are the characteristic admittances of J-inverters and Y_0 is the characteristic admittance of the terminating lines. To realize the J-inverters obtained above, the even and odd mode characteristic impedances of the coupled microstrip line resonators are determined by

$$\left(Z_{0e}\right)_{j,j+1} = \frac{1}{Y_0}\left[1 + \frac{J_{j,j+1}}{Y_0} + \left(\frac{J_{j,j+1}}{Y_0}\right)^2\right] \qquad j = 0 \text{ to } n$$

$$\left(Z_{0o}\right)_{j,j+1} = \frac{1}{Y_0}\left[1 - \frac{J_{j,j+1}}{Y_0} + \left(\frac{J_{j,j+1}}{Y_0}\right)^2\right] \qquad j = 0 \text{ to } n$$

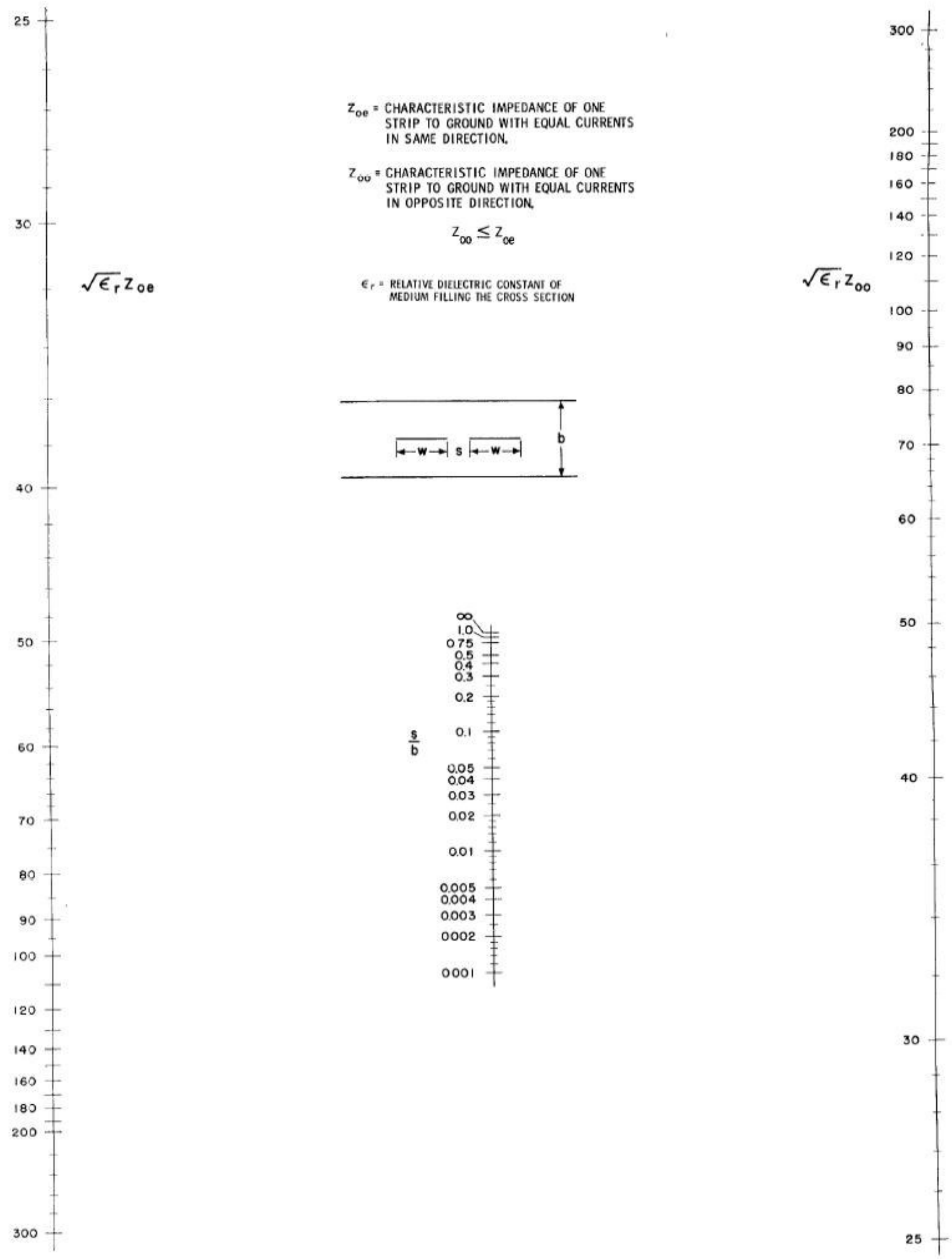
Z_{oe} = CHARACTERISTIC IMPEDANCE OF ONE STRIP TO GROUND WITH EQUAL CURRENTS IN SAME DIRECTION.
Z_{oo} = CHARACTERISTIC IMPEDANCE OF ONE STRIP TO GROUND WITH EQUAL CURRENTS IN OPPOSITE DIRECTION.
$Z_{oo} \leq Z_{oe}$
ϵ_r = RELATIVE DIELECTRIC CONSTANT OF MEDIUM FILLING THE CROSS SECTION
$\sqrt{\epsilon_r} Z_{oe}$
$\sqrt{\epsilon_r} Z_{oo}$
$\frac{s}{b}$
w
s
b

(a)

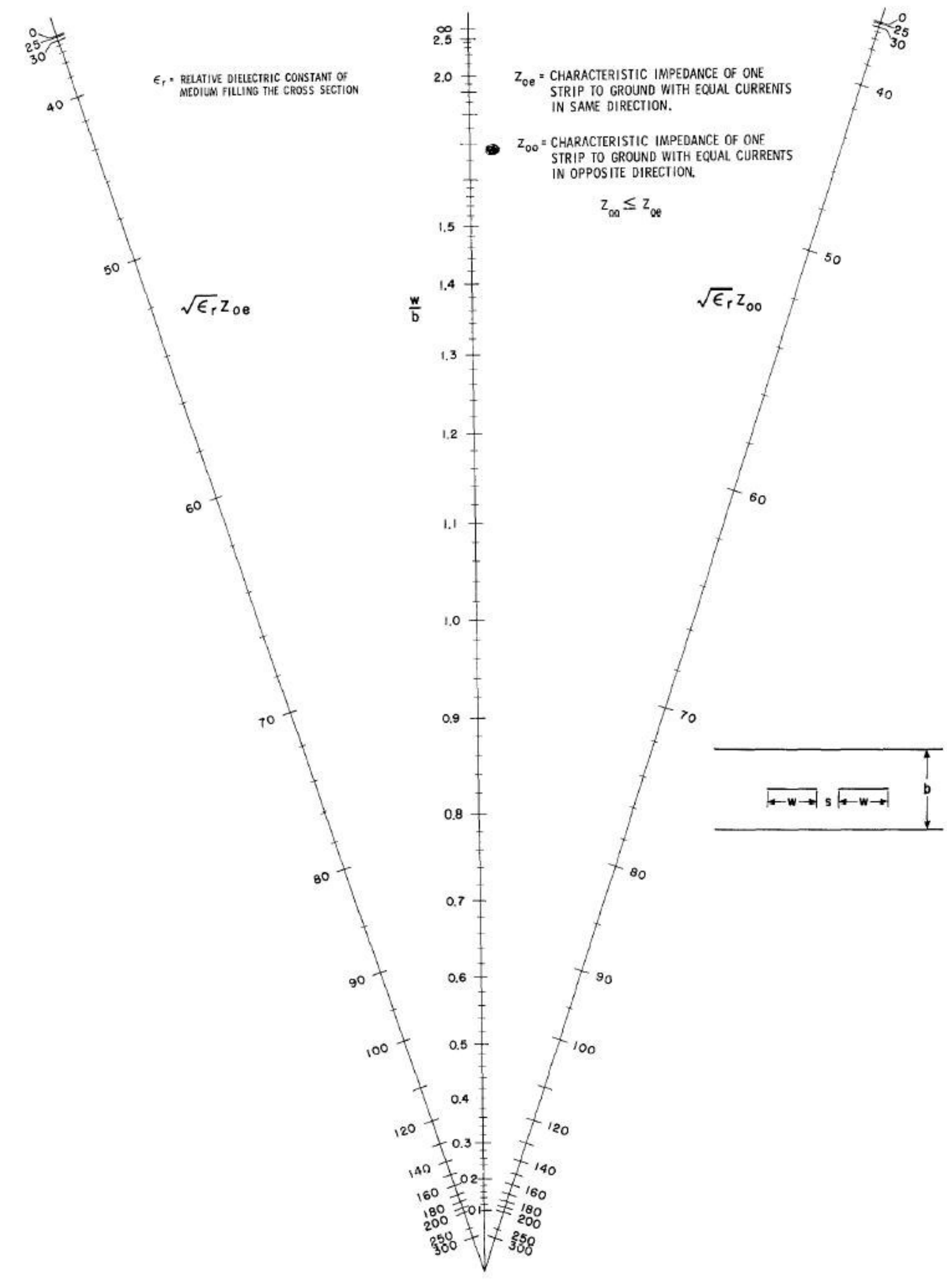

(b)

Fig. 4.19 Graphs to determine the dimensions of coupled line (a) Spacing (b) Width

The dimensions of the filter structure are determined with the help of the two graphs shown in Fig. 4.19 and using the even and odd mode impedance values as described above. Some care must be taken using these for microstrip lines as they were defined for strip lines parameter ‘b’, ground plane spacing have to be replaced with 2h (where h is the dielectric height on which filter structure have to be fabricated). Length of each coupled line section is of quarter wavelength as the wavelength depends on the width of the microstrip line in the coupled line section it will be different for each section. Actual microstrip line length are shortened by the amount $d_{j,j+1}$ which has been found to be constant of 0.33h which is apparently satisfactory.

Example 4.4

Design a 3rd order 0.5dB equi-ripple Chebyshev band pass filter at a center frequency 2GHz, 10% bandwidth and assume filter impedance Z_0=50ohm. What is the attenuation at 1.8GHz? Use FR4 substrate for filter implementation.

Solution:

f_0=2GHz, Δ=0.1, Z_0=50ohm

As in the previous example 11.2, g_0=1, g_1=1.5963, g_2=1.0967, g_3=1.5963, g_4=1. Note that g values are dependent only on the order of the filter and the passband ripple.

$$\frac{J_{0,1}}{Y_0}=\sqrt{\frac{\pi}{2}\frac{\Delta}{g_0g_1}}=0.3137$$

$$\frac{J_{1,2}}{Y_0}=\frac{\pi\Delta}{2}\frac{1}{\sqrt{g_1g_2}}=0.1187$$

$$\frac{J_{2,3}}{Y_0}=\frac{\pi\Delta}{2}\frac{1}{\sqrt{g_2g_3}}=0.1187$$

$$\frac{J_{3,4}}{Y_0}=\sqrt{\frac{\pi}{2}\frac{\Delta}{g_3g_4}}=0.3137$$

$$(Z_{0e})_{0,1} = \frac{1}{Y_0}\left[1 + \frac{J_{0,1}}{Y_0} + \left(\frac{J_{0,1}}{Y_0}\right)^2\right] = 70.6 = (Z_{0e})_{3,4}$$

$$(Z_{0o})_{0,1} = \frac{1}{Y_0}\left[1 - \frac{J_{0,1}}{Y_0} + \left(\frac{J_{0,1}}{Y_0}\right)^2\right] = 39.23 = (Z_{0e})_{3,4}$$

$$(Z_{0e})_{1,2} = \frac{1}{Y_0}\left[1 + \frac{J_{1,2}}{Y_0} + \left(\frac{J_{1,2}}{Y_0}\right)^2\right] = 56.6 = (Z_{0e})_{2,3}$$

$$(Z_{0o})_{1,2} = \frac{1}{Y_0}\left[1 - \frac{J_{1,2}}{Y_0} + \left(\frac{J_{1,2}}{Y_0}\right)^2\right] = 44.77 = (Z_{0e})_{2,3}$$

Therefore,

$$\sqrt{\varepsilon_r}\,(Z_{0e})_{0,1} = \sqrt{\varepsilon_r}\,70.6 = 148.09 = \sqrt{\varepsilon_r}\,(Z_{0e})_{3,4}$$
$$(Z_{0o})_{0,1} = \sqrt{\varepsilon_r}\,39.23 = 82.29 = \sqrt{\varepsilon_r}\,(Z_{0e})_{3,4}$$
$$(Z_{0e})_{1,2} = \sqrt{\varepsilon_r}\,56.6 = 118.8 = \sqrt{\varepsilon_r}\,(Z_{0e})_{2,3}$$
$$(Z_{0o})_{1,2} = \sqrt{\varepsilon_r}\,44.77 = 93.91 = \sqrt{\varepsilon_r}\,(Z_{0e})_{2,3}$$

For a 50ohm line at 2GHz, A=1.529, W_m/h=1.819, W_m=2.91mm.

From graph in Fig. 4.19 (a), we can read the values of spacing by drawing a line from $\sqrt{\varepsilon_r}\,(Z_{0e})_{0,1}$ to $\sqrt{\varepsilon_r}\,(Z_{0e})_{0,1}$ and noting down the value of s/b where this line crosses that will give the value of s_1/b= s_4/b=0.12. Similarly, s_2/b= s_3/b=0.35. Therefore, s_1 = s_4 =0.12×2×1.6mm=0.384mm and s_2 = s_3 =0.35×2×1.6mm=1.12mm. From graphs in Fig. 4.19(b), we can also read the values of w_1 = w_4 =0.38×2×1.6mm=1.216mm and w_2 = w_3 =0.45×2×1.6mm=1.44mm (by applying the same method as above). Length of each section l can be calculated as $\frac{\lambda_g}{4} - 2d \cong \frac{\lambda}{4\sqrt{\varepsilon_r}} - 0.33h = 17.3mm$. L can be taken as 10mm. Refer to Fig. 4.18 for the dimensions specified here.

Example 4.5

Design a 3rd order 0.1dB equi-ripple Chebyshev GSM band pass filter (890MHz to 960MHz) of 10% bandwidth to attain 23dB attenuation at 870MHz. Use FR4 substrate for filter implementation.

Solution:

The parallel coupled microstip line band pass filter is designed on an FR4 substrate of relative dielectric constant 4.4 and thickness of 1.6mm. The midband frequency of the first passband is taken 900MHz which covers the GSM band of frequencies which ranges from 890MHz to 960MHz. Here the type of the filter chosen for this design is Chebyshev third order filter and the dimensions of all coupled lines are given in Fig. 4.20 (a) The feeding lines at input and output ports are a 50Ω lines and length of lines are chosen as 10.0mm.

1

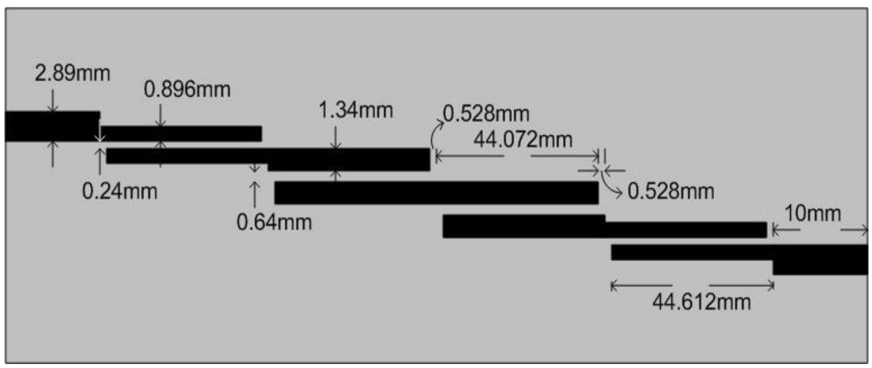

(a)

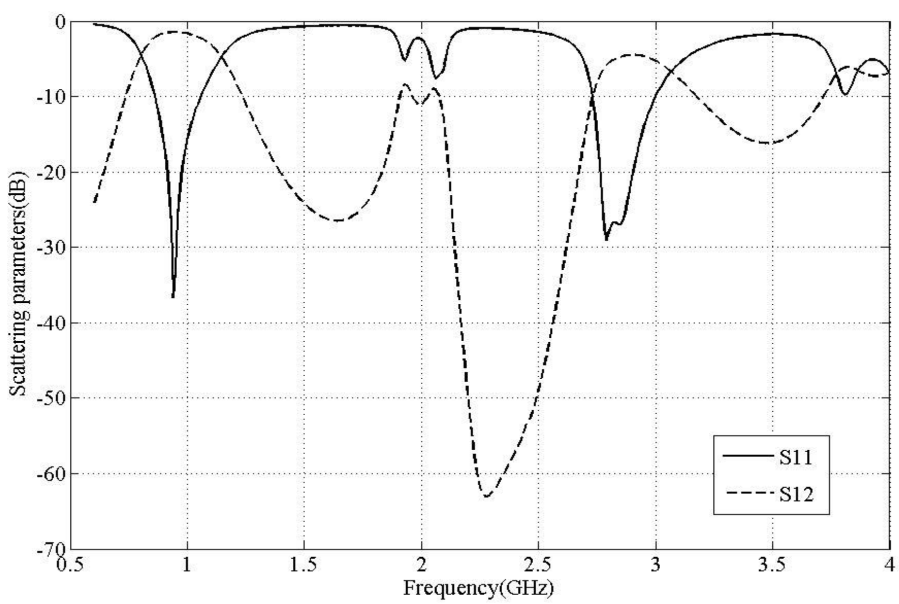

(b)

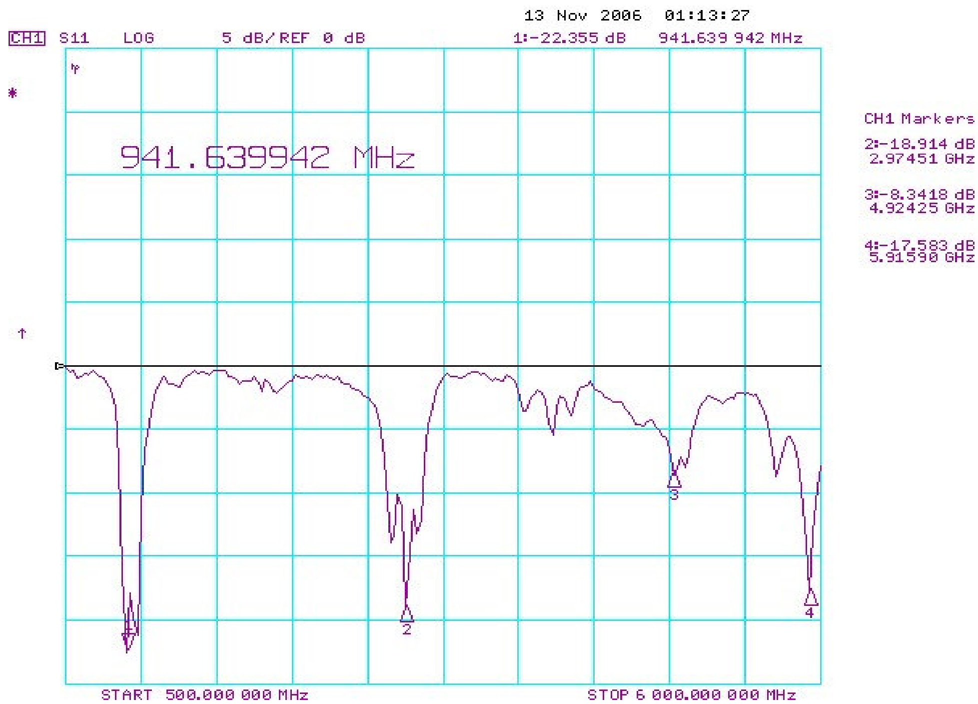

(c)

Fig. 4.20 PCML band pass filter (a) Design layout (b) Simulated results (c) Fabrication results

Fig. 4.20 (b) shows the simulation results of the parallel coupled resonator microstrip line band pass filter designed having the dimensions shown in Fig. 4.20 (a). Scattering parameters (S_{11} and S_{12}) are observed in the frequency range from 0.5GHz to 4GHz by simulating the band pass filter. The results shows a passband at 940MHz and the passband ranging from 860MHz to 1060MHz with a passband width of 200MHz. Fig. 4.20 (c) shows the results of the same filter has been designed and fabricated, which exactly comparable with the simulation results shown in Fig. 4.20 (b).

4.3 Power Dividers and Directional Couplers

4.3.1 Power Dividers

Power dividers are used in microwave frequencies because usually we have only one microwave source and we need to input this single source to many microwave devices in a microwave device network. Similarly we require power combiners to combine the microwave power from many devices for many practical applications. We can use the same power divider as a power combiner if we interchange the output ports and input ports. In microwave frequencies, the modeling of the circuits is different from the expected lumped model. Therefore, power dividers in microwave frequencies are not just resistive power dividers as in the low frequency or DC model.

The important issues while using power dividers are the specifications or properties of the dividers. In microwave frequency applications, for example power can be reflected from the output ports. Then to avoid the reflected power, power divider should satisfy the maximum power transfer theory, which says that the impedance of the load should be the complex conjugate of the impedance seen from the load end when load is not connected. This is called "*matching*" of the ports. This leads to maximum transfer of power to the load and because of no reflection, avoid burning out the power supply. Also, again for maximal power transfer to the output ports, the network should not dissipate power and this property is called "*lossless*". Another important issue is the “*isolation”* of the output ports, any unwanted signal coming from the output ports should not go to the other output lines. All these will be clear when we discuss the following power divider types.

There are three types of power dividers:

1) Lossless Y-Junction Power Divider
2) Lossy (Resistive) Y-Junction Power Divider
3) Equal/Unequal Split Quadrature (Wilkinson) Power Divider

Review Question 4.1 What are the objectives for designing Power Dividers?

Answer: power division, matched ports, lossless networks and output port isolation

Review Question 4.2 What are three types of power dividers?

Answer: Lossless Y-Junction, Lossy (Resistive) Y-Junction and Equal/Unequal Split Quadrature (Wilkinson) Power Divider

4.3.1.1 Lossless Y-Junction Power Divider

A microstrip Y-Junction lossless power divider is depicted in Figure 4.21 (a) and its equivalent circuit is drawn in Fig. 4.21 (b). It takes the shape of Y and hence the common name Y-junction power divider. Due to fringing fields and higher order modes excitation at the junction, the susceptance B in Figure 4.21 (b) is not negligible. But for practical applications we can add some types of reactive elements to cancel this susceptance. In that case, Y_{in} looking into the junction as shown in Figure 4.21(b) will be given as: $Y_{in}=1/Z_1=1/Z_2+1/Z_3$.

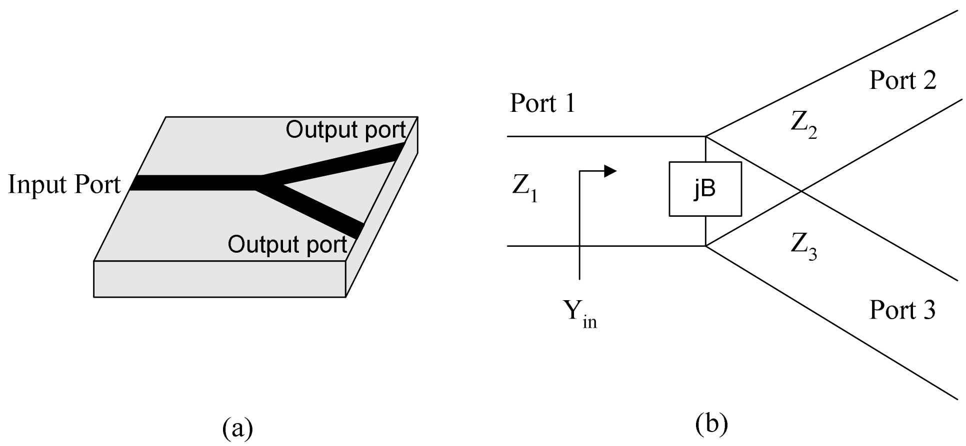

Figure 4.21 A lossless Y-Junction Power Divider (a) Geometry (b) Equivalent circuit

Note that the output line impedances Z_2 and Z_3 can be chosen to get various power division ratios. For instance, a 3 dB (equal split) power divider can be achieved by using two 100 Ω output lines when the input impedance has a 50 Ω characteristic impedance. And quarter-wave transformers can be used to make the output lines to 50 Ω lines since the microwave networks generally has 50 Ω as impedance, otherwise there will be a impedance mismatch with the external microwave devices. With this power divider we have achieved our aim of power division but the other two issues of impedance mismatch and isolation still remain. In the next sub-section, we will try to analyze the lossy (resistive) power dividers which will satisfy some of our specifications for power divider.

Review Question 4.3 Has the lossless Y-junction power divider achieve impedance matching and output port isolation?

Answer: No

Example 4.6 A lossless Y-Junction power divider has input line of characteristic impedance 50 Ω. Calculate the output lines characteristic impedance to achieve power division of 2:3 and what are the reflection coefficients at the output ports.

Solution:

Power division ratio to achieve is P_2: P_3 = 2: 3 Therefore P_1: P_2: P_3 = 1: 2/5 : 3/5 = $1/Z_1$: $1/Z_2$: $1/Z_3$ implies $Z_2 = 5/2\ Z_1$ = 125 Ω and $Z_3 = 5/3\ Z_1 = 83.3$ Ω. So looking from the port 1 it sees an impedance of 50 Ω. Looking from port 2, the impedance is $Z_1 \parallel Z_3$ =31.24 Ω and looking from port 3, the impedance is $Z_1 \parallel Z_2$ = 35.7 Ω. Hence Γ_2 = (31.24-125)/(31.24+125)= -0.6 and Γ_3 = (35.7-83.3)/(35.7+83.3)= -0.4.

4.3.1.2 Lossy (Resistive) Y-Junction Power Divider

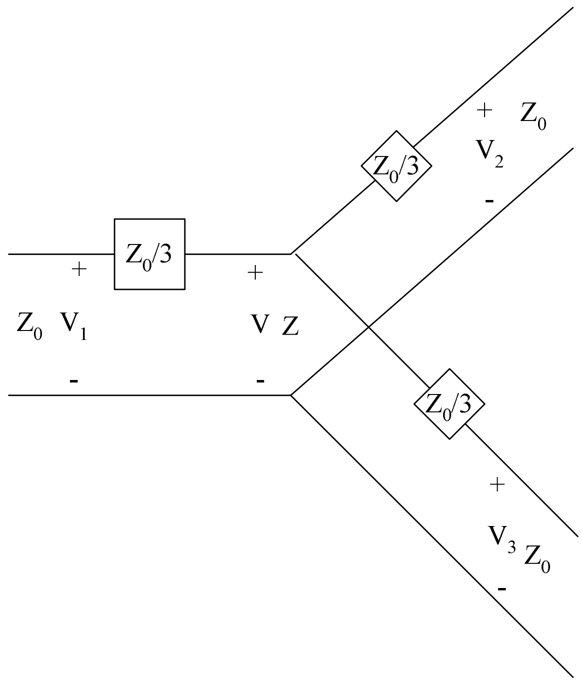

Figure 4.22 A lossy (resistive) Y-Junction Power Divider

For such lossy Y-junction power divider the impedance Z looking into one of the output arms is $Z = Z_0/3+Z_0 = (4/3)\ Z_0$. Since the two output arms are in parallel connection, the total impedance for the two output arms is $(2/3)\ Z_0$. Therefore the impedance seen from the input port is Z_0. Hence $s_{11} = 0$ and similarly due to symmetry $s_{22} = s_{33} = 0$. The voltage V at the junction is given by $[V_1\ \{(2/3)\ Z_0\ \}]\ /\ Z_0$ and V_2 and V_3 are given by $V_2 = V_3 = V\ Z_0\ /\ (Z_0 + Z_0\ /3) = ¾\ V = ½\ V_1$. Hence due to symmetry $s_{21} = s_{31} = s_{23} = ½$. And since the network is reciprocal, we have $[s]=\frac{1}{2}\begin{bmatrix}0 & 1 & 1\\ 1 & 0 & 1\\ 1 & 1 & 0\end{bmatrix}$

Therefore the power input to the power divider is $P_{in} = \{½\ (V_1)^2\ \}/\ Z_0$ and $P_2 = P_3 = ½\ (1/2\ V_1)^2\ /\ Z_0 = (1/8\ V_1^2\ )\ /\ Z_0 = ¼\ P_{in}$ which shows that half the power is dissipated in resistors.

Review Question 4.4 If the power input to a lossy (resistive) Y-junction power divider is P_{in}, then what are the P_{out} at the two output ports?

Answer: P_{out} =1/4 P_{in} since half the power is dissipated in the lossy resistors of the power divider.

Review Question 4.5 Is the output ports matched and isolated for lossy (resistive) Y-junction power divider?

Answer: Output ports are matched but they are not isolated.

4.3.1.3 Equal/Unequal Split Quadrature (Wilkinson) Power Divider

Equal/Unequal Split Quadrature (Wilkinson) Power Divider achieves all the criteria of a power divider, i.e., lossless, isolation and matching along with power division. In this power divider, there are four different sections namely (a) input port (b) quarter-wave transformer (c) isolation resistors (d) output ports.

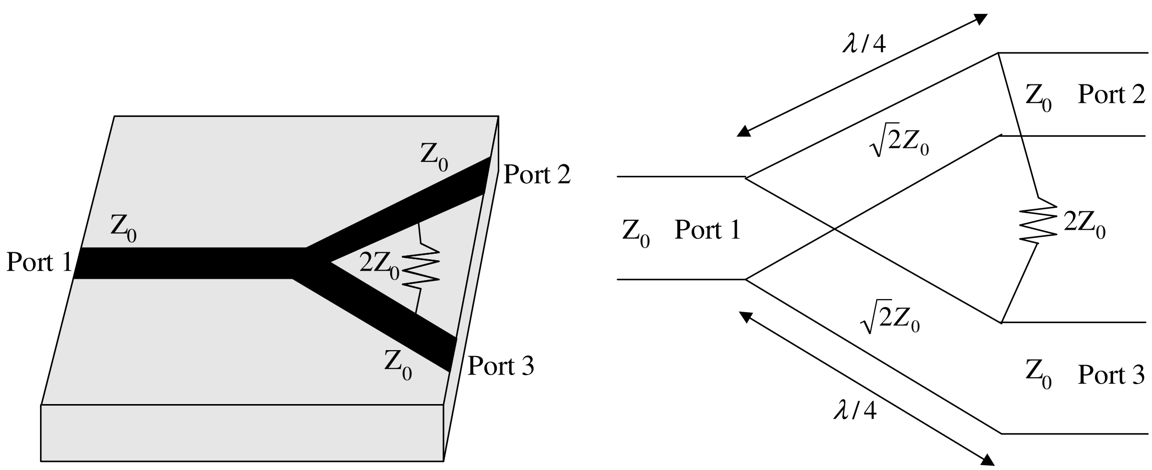

(a) (b)

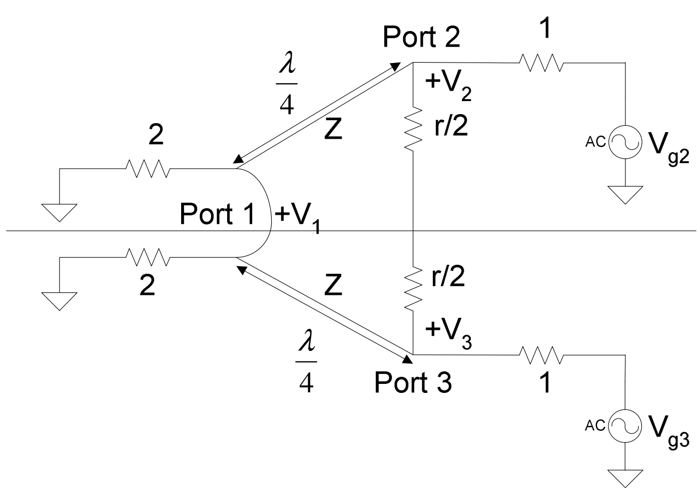

(c)

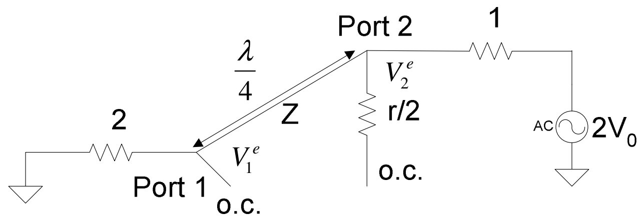

(d)

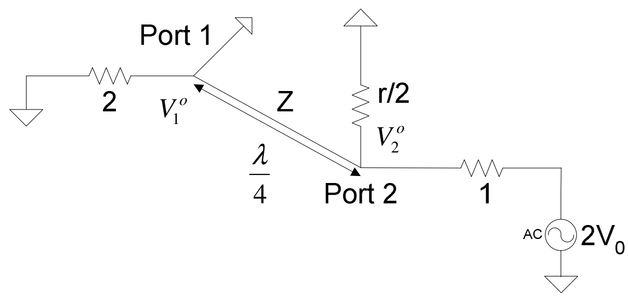

(e)

Figure 4.23 Equal Split Quadrature (Wilkinson) Power Divider (a) Geometry (b) Equivalent circuit (c) Normalized and symmetric form (d) Even-mode excitation (e) Odd-mode excitation

How to find s_{11}?

The question is why we need quarter-wave transformers and isolation resistors. Consider the case when the power is coming from input port 1 and the output ports 2 and 3 are terminated with matched loads. Since voltage at the two output ports are equal in phase and amplitude, no current flows through isolation resistors ($2Z_0$). The isolation resistor cannot pass any current on it and this means that it can be removed from the analysis of the network. $Z_{in}(1) = \frac{1}{2} Z_0 (Z_L+jZ_0\tan\beta l)/(Z_0+jZ_L\tan\beta l)$ is the impedance seen from port 1 where Z_L is Z_0 and Z_0 is $\sqrt{2} Z_0$. Since $l=\lambda/4$, $\beta l=\pi/2$, $\tan\beta l \rightarrow \infty$. $Z_{in}(1) = \frac{1}{2} (Z_0)^2/Z_L = \frac{1}{2} (\sqrt{2}Z_0)^2/Z_0 = Z_0$. This means that the input impedance is matched to the whole circuit. Thus the reflected power for the input port 1 is zero ($s_{11}=0$). Similarly due to symmetry, $s_{22}=0$ and $s_{33}=0$.The quarter-wave transformer part leads to the matched ports.

Output ports isolation:

Isolator resistor is to isolate the output ports. If there is a coupling effect between output ports or in other words the power comes from an output port has an effect on the other output ports, the perfect division of power cannot be possible. This isolation port avoids the coupling effects of the output ports. When a signal enters from port 1 it is split into equal amplitude and equal phase output signals at ports 2 and 3. Since each end of the isolation resistor between ports 2 and 3 is at the same potential no current flows through it and therefore the resistor is decoupled from the input. Note that a signal input at either port 2 or 3, half the power is dissipated in the resistor and half the power is delivered to load 1. A signal entering from port 2 is split and part of it goes through the isolation resistor and remaining part goes through the upper arm of the power divider. Both these signals will again recombine at port 3, but they are equal in amplitude and 180^0 degrees out of phase. This is difficult to see with the simple network analysis so let us apply even-odd mode analysis for this.

The Wilkinson power divider shown in Fig. 4.23 is a three port network that is matched on all ports, but is lossy. The Wilkinson divider also provides output port isolation (S_{23}=S_{32}=0). Analyzing this network directly to find its S-parameters would require the solution of many simultaneous equations. The amount of work required to find the S-parameters of this and other similar networks is greatly simplified by the use of the even/odd mode analysis technique. Finding the S-parameters with a source at port 1 is relatively straightforward. It is more difficult to find the S-parameters with an input wave on port 2 or port 3. We will first consider the case of a source at port 2. As we will have to redraw the network several times, we will use a single wire to represent transmission lines to make the picture simpler. If we add the results, we have the voltages for the original single source. *Because of the symmetry of the new network with even or odd sources, the analysis is much easier than is the case for the original source on port 2.* Note that we have used normalized resistances or impedances in the Fig. 4.23 (c) since it makes us easy in the analysis.

Even Mode

For even mode excitation (refer to Fig. 4.23 (d)), V_{g2}=V_{g3}=$2V_0$. Therefore, $V_2^e = V_3^e$ and no current flows through r/2 and at the port 1 connection. Thus we can separate the network with o.c. at these points. Looking into port 2, $Z_2^e = \frac{Z^2}{2} \because Z = \sqrt{2} \Rightarrow Z_2^e = 1 \Rightarrow V_2^e = V_0$. Let us take x=0 at port 1 then at port 2 x=-λ/4.

$$\therefore V(x) = V^+(e^{-j\beta x} + \Gamma e^{j\beta x})$$

$$\Rightarrow V_2^e = V(-\lambda/4) = jV^+(1-\Gamma) = V_0$$

$$\Rightarrow V_1^e = V(0) = V^+(1+\Gamma) = j\frac{V_0(\Gamma+1)}{\Gamma-1} \because \Gamma = \frac{2-\sqrt{2}}{2+\sqrt{2}}$$

$$\Rightarrow V_1^e = -jV_0\sqrt{2}; V_2^e = V_0 = V_3^e$$

Note that due to even symmetry we can observe that $V_2^e = V_3^e$.

Odd Mode

For odd mode excitation (refer to Fig. 4.23 (e)), V_{g2}=-V_{g3}=$2V_0$, so $V_2^o = -V_3^o$ the line of symmetry through the middle of the network must be an equi-potential at 0V, so we can separate the network into two by grounding at the two points of the mid plane. Looking into port 2,

$$Z_2^0 = Z_{in} \,||\, \frac{r}{2} = \frac{Z^2}{Z_L = 0} \,||\, \frac{r}{2} = \infty \,||\, \frac{r}{2} = \frac{r}{2} \because r = 2 \Rightarrow Z_2^0 = 1 \Rightarrow V_2^0 = V_0; V_1^0 = 0; V_3^0 = -V_0$$

Note that due to odd symmetry we an observe that $V_2^0 = -V_3^0$.

Superposition

We can now combine the voltages for the even and odd excitations using principle of superposition for the excitation at port 2:

$$S_{12} = \frac{V_1^e + V_1^o}{V_2^e + V_2^o} = \frac{-jV_0\sqrt{2}+0}{V_0 + V_0} = -\frac{j}{\sqrt{2}}$$

$$S_{32} = \frac{V_3^e + V_3^o}{V_2^e + V_2^o} = \frac{0}{2V_0} = 0$$

Similarly we could also find other scattering parameters. For those cases, we need to choose the source excitation accordingly. $S_{13}=S_{12}$ because port 2 and 3 are symmetric. Also $S_{32}=S_{23}$ because port 2 and 3 are symmetric. Note for excitation at port 3, the power divider circuit will have the similar scattering performance to that of the excitation at port 2. For port 1 excitation, we could analyze the power divider circuit in the similar way we have done for calculation of s_{11} at the start of this sub-section. If some power is fed at port 1, half of them will go to port 2 and remaining half will go to port 3. And the quarter-wave transformer will give a phase shift of 90 degrees for port 2 and 3, hence, we can find the S_{31} and S_{21} easily.

Equal Split Quadrature (Wilkinson) Power Divider can be generalized to N-way divider or combiner as depicted in Figure 4.24. This power divider has the matched and isolated output ports. For N=3 case, there are two ways to realize isolation resistors connections: "star" and "delta" configurations.

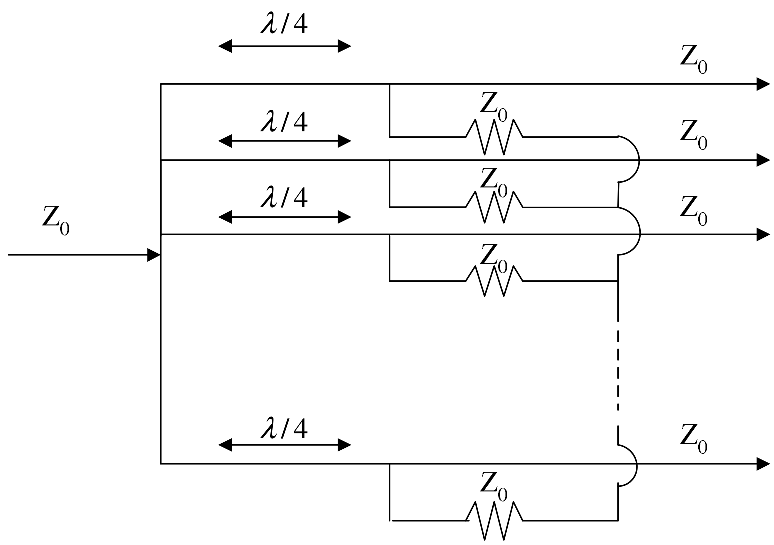

Figure 4.24 Equal Split Quadrature N-way (Wilkinson) Power Divider

The way to make power split unequally requires two things: the quarter wave sections must be of different impedances, to encourage more of signal to travel in/out of the lower impedance arm. Note that the output lines are matched to $Z_2=nZ_0$ and $Z_3=Z_0/n$ and when n=1 it becomes equal split Wilkinson power divider. So a second set of quarter-wave sections are needed to transform the arm impedances back to 50Ω. Unequal Split (Wilkinson) Power Divider can also be designed using the following design equations:

$$Z_{03} = Z_0\sqrt{\frac{1+n^2}{n^3}}; Z_{02} = n^2 Z_{03} = Z_0\sqrt{n(1+n^2)}; Z = Z_0(n+\frac{1}{n})$$

These set of equations when satisfied ensure that the ports will be matched and port 2 and 3 will be isolated. With the second set of quarter-wave transformers, which are used for impedance matching for output arms, it looks like a two-stage Wilkinson power dividers (second set of quarter-wave transformers are not shown in Figure 4.25).

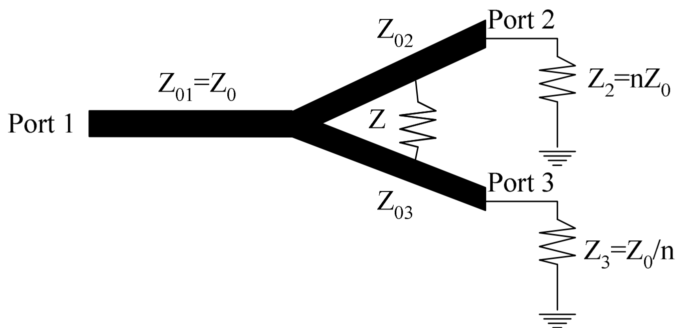

Figure 4.25 Unequal Split Quadrature (Wilkinson) Power Divider

4.3.2 Branch Line Couplers

Generally branch-line couplers are 3dB, four ports directional couplers having a 90° phase difference between its two output ports named “through” and “coupled” arms. Branch-line couplers (also named as Quadrature Hybrid) are often made in microstrip or stripline form.

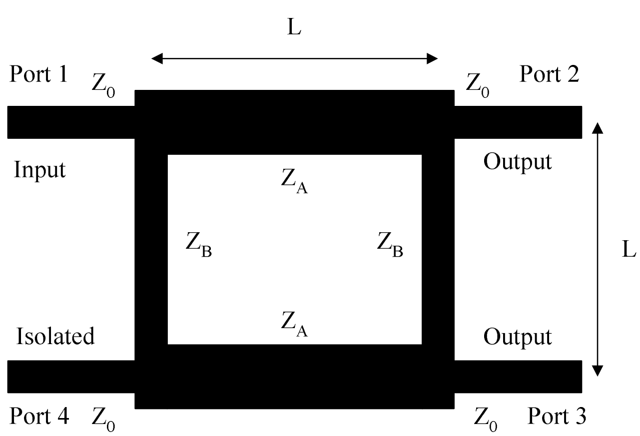

Figure 4.26 Branch line coupler

4.3.2.1 Design of Branch Line Couplers

The geometry of the branch line coupler is shown in Figure 4.26. A branch line coupler is made by two main transmission lines, which are shunt-connected by two secondary branch lines. As it can be seen from the figure, it has a symmetrical four port. First port is named as input port, second and third ports are output ports and the fourth port is the isolated port. The second port is also named as direct or through port and the third port is named as coupled port. It is obvious that due to the symmetry of the coupler any of these ports can be used as the input port but at the same time the output ports and isolated port changes accordingly. When we analyze the scattering matrix of this coupler we will also see the result of that symmetry in scattering matrix. Considering the dimensions of the coupler the length of the branch line and series line is generally chosen as one fourth of the design wavelength. As it is shown in Figure 4.26, if we name the length of series and stub transmission lines as L then L can be found as: $L = \lambda/4 = v_p/(4f) = c/(4f\sqrt{\varepsilon_r})$.

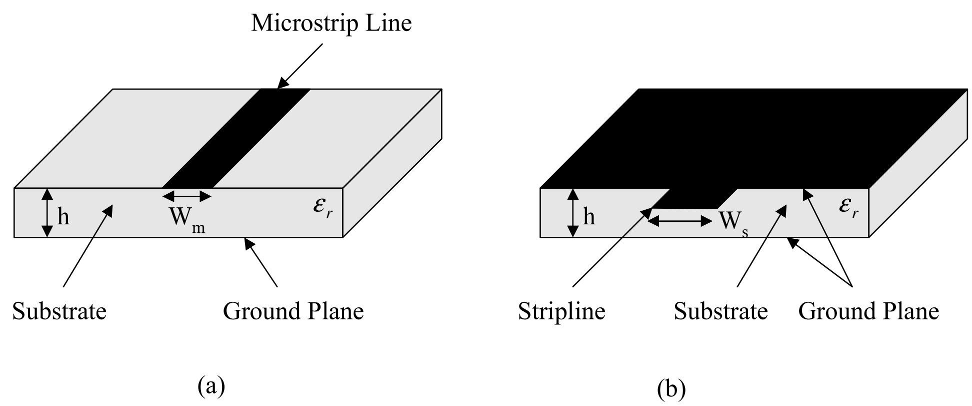

Figure 4.27 Geometry of (a) microstrip line and (b) stripline used in Branch-line coupler

We generally design branch-line couplers in two forms: Microstrip line and Stripline. Geometry of the microstrip line and stripline can be seen from Figure 4.27. According to the impedance choice of the series and stub microstrip transmission lines we can calculate the W_m/h ratios of those lines in microstrip form by using the following formulae:

Given ε_r and Z_0

$$\frac{W_m}{h} = \begin{cases} \dfrac{8e^A}{e^{2A}-2}; \dfrac{W_m}{h} < 2 \\ \dfrac{2}{\pi}\left[B - 1 - \ln(2B-1) + \dfrac{\varepsilon_r - 1}{2\varepsilon_r}\left\{\ln(B-1) + 0.39 - \dfrac{0.61}{\varepsilon_r}\right\}\right]; \dfrac{W_m}{h} > 2 \end{cases}$$

where $A = \dfrac{Z_0}{60}\sqrt{\dfrac{\varepsilon_r + 1}{2}} + \dfrac{\varepsilon_r - 1}{\varepsilon_r + 1}\left(0.23 + \dfrac{0.11}{\varepsilon_r}\right); B = \dfrac{377\pi}{2Z_0\sqrt{\varepsilon_r}}$

Considering the stripline branch line coupler design, we can calculate W_s/h ratios for each series and shunt transmission line in the branch line coupler using the following formulae:

$$\frac{W_s}{h} = \begin{cases} \dfrac{30\pi}{\sqrt{\varepsilon_r} Z_0} - 0.441; \sqrt{\varepsilon_r} Z_0 < 120 \\ 0.85 - \sqrt{0.6 - \dfrac{30\pi}{\sqrt{\varepsilon_r} Z_0} - 0.441}; \sqrt{\varepsilon_r} Z_0 > 120 \end{cases}$$

4.3.2.2 Analysis of Branch Line Couplers

Even and odd mode analysis and s-parameters

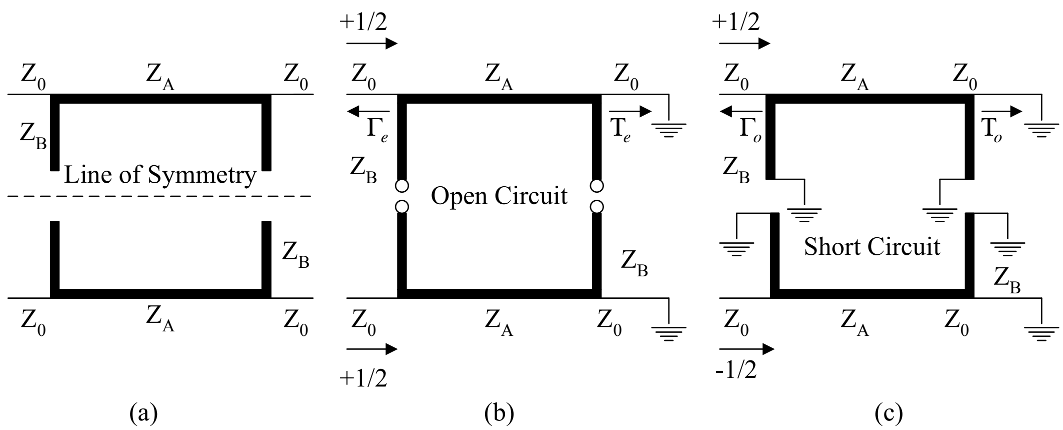

Figure 4.28 (a) Line of Symmetry (b) Even mode analysis (c) Odd mode analysis

In the analysis of branch-line coupler in order to find the scattering matrix of the coupler, we use even and odd mode analysis. In both these modes, we divide the branch-line coupler symmetrically as in the Figure 4.28 (a). Generally considering that we give V voltage to the input port. In even mode analysis, 1/2 of it goes to the input port and rest to the isolated port and for the odd mode analysis, 1/2 of it goes to the input port and –1/2 of it goes to the isolated port. Furthermore, for the even mode, we assume that the stubs of the divided circuit are open circuited and for the odd mode they are short circuited as illustrated in Figure 4.28 (b) and (c). For this analysis, if we consider the superposition of the incoming voltage, it results as V voltage to the input and 0 voltage to the isolated port. Furthermore we have for each mode incident and reflected waves, for even mode it is illustrated in the Figure 4.28 (b). As it is seen we have an incident wave 1/2 of the actual voltage and at first stub we have a reflection having a reflection coefficient Γ_e and at second port a transmitted signal having transmission coefficient Te. Considering the contribution of the even mode to the port waves for first port we have $1/2V\Gamma_e$, for second port we have $1/2VT_e$, for third port $1/2VT_e$, and for the fourth port $1/2V\Gamma_e$ (Note the port numbering from Fig. 4.26). In addition, for the odd mode incident and reflected waves are illustrated in the Figure 4.28 (c). As it is seen we have an incident wave 1/2 of the actual voltage at first port and −1/2 of it at fourth port as incoming wave. Also at first stub we have a reflection having a reflection coefficient Γ_o and at second port a transmitted signal having transmission coefficient T_o. Considering the contribution of the odd mode to the port waves for first port we have $1/2V\Gamma_o$, for second port we have $1/2VT_o$, for third port $-1/2VT_o$, and for the fourth port $-1/2V\Gamma_o$. At this point, we express the emerging wave at each port of the branch-line coupler as the superposition of the even and odd mode waves as following:

$B_1=(1/2\Gamma e+1/2\Gamma_o)V$, $B_2=(1/2T_e+1/2T_o)V$, $B_3=(1/2T_e-1/2T_o)V$, $B_4=(1/2\Gamma_e-1/2\Gamma_o)V$

The ABCD matrix is used to find the overall transmission and reflection characteristics of the network. Having $Y_A=1/Z_A$ and $Y_B=1/Z_B$ we have the ABCD matrix of even and odd mode. For even mode ABCD parameters are as following:

$$\begin{bmatrix} A & B \\ C & D \end{bmatrix}_e = \begin{bmatrix} A & B \\ C & D \end{bmatrix}_{o.c.stub} \begin{bmatrix} A & B \\ C & D \end{bmatrix}_{line} \begin{bmatrix} A & B \\ C & D \end{bmatrix}_{o.c.stub}$$

For o. c. shunt stub of length l/2, $Z_{in}=Z_0/(j\tan\beta l/2)$ hence $Y_{in}= jY_0\tan(\beta l/2)$.

$$\begin{bmatrix} A & B \\ C & D \end{bmatrix}_e = \begin{bmatrix} 1 & 0 \\ jY_B & 1 \end{bmatrix} \begin{bmatrix} \cos\beta l & jZ_A\sin\beta l \\ jY_A\sin\beta l & \cos\beta l \end{bmatrix} \begin{bmatrix} 1 & 0 \\ jY_B & 1 \end{bmatrix}$$

Since we have $l=\lambda/4$ at our design frequency, $\beta l=(2\pi/\lambda)*(\lambda/4)=\pi/2$. Therefore, $\cos\beta l=0$ and $\sin\beta l=1$ and the ABCD matrix then becomes:

$$\begin{bmatrix} A & B \\ C & D \end{bmatrix}_e = \begin{bmatrix} 1 & 0 \\ jY_B & 1 \end{bmatrix} \begin{bmatrix} 0 & jZ_A \\ jY_A & 0 \end{bmatrix} \begin{bmatrix} 1 & 0 \\ jY_B & 1 \end{bmatrix} = \begin{bmatrix} -Y_BZ_A & jZ_A \\ j\left(Y_A - Y_B^2Z_A\right) & -Y_BZ_A \end{bmatrix}$$

For the odd mode ABCD matrix:

$$\begin{bmatrix} A & B \\ C & D \end{bmatrix}_0 = \begin{bmatrix} A & B \\ C & D \end{bmatrix}_{s.c.stub} \begin{bmatrix} A & B \\ C & D \end{bmatrix}_{line} \begin{bmatrix} A & B \\ C & D \end{bmatrix}_{s.c.stub}$$

For s. c. shunt stub of length l/2, $Z_{in}=jZ_0\tan\beta l/2$ hence $Y_{in}= -jY_0/(\tan(\beta l/2))$.

$$\begin{bmatrix} A & B \\ C & D \end{bmatrix}_0 = \begin{bmatrix} 1 & 0 \\ -jY_B & 1 \end{bmatrix} \begin{bmatrix} \cos\beta l & jZ_A\sin\beta l \\ jY_A\sin\beta l & \cos\beta l \end{bmatrix} \begin{bmatrix} 1 & 0 \\ -jY_B & 1 \end{bmatrix}$$

Since we have $l=\lambda/4$ and so $\beta l=(2\pi/\lambda)*(\lambda/4)=\pi/2$. Therefore, $\cos\beta l=0$ and $\sin\beta l=1$ and the ABCD matrix then becomes

$$\begin{bmatrix} A & B \\ C & D \end{bmatrix}_0 = \begin{bmatrix} 1 & 0 \\ -jY_B & 1 \end{bmatrix} \begin{bmatrix} 0 & jZ_A \\ jY_A & 0 \end{bmatrix} \begin{bmatrix} 1 & 0 \\ -jY_B & 1 \end{bmatrix} = \begin{bmatrix} Y_B Z_A & jZ_A \\ j\left(Y_A - Y_B^2 Z_A\right) & Y_B Z_A \end{bmatrix}$$

At that point we can find Γ_e, Γ_o, T_e, T_o by using the following equations:

$$\Gamma_e = \frac{(A-D)+(BY_0-CZ_0)}{(A+D)+(BY_0+CZ_0)}; T_e = \frac{2}{(A+D)+(BY_0+CZ_0)};$$
$$\Gamma_0 = \frac{(A-D)+(BY_0-CZ_0)}{(A+D)+(BY_0+CZ_0)}; T_0 = \frac{2}{(A+D)+(BY_0+CZ_0)}$$

Then solving above equations with parameters of even and odd mode ABCD matrices at center frequency where $f=\nu_p/\lambda=\nu_p/4L$ are given by:

$$\Gamma_e = \frac{Z_A^2 Y_0^2 - Z_0^2\left(Y_A - Y_B^2 Z_A\right)^2 - j\left(2Y_B Z_A\left(Z_A Y_0 - Y_A Z_0 + Y_B^2 Z_A Z_0\right)\right)}{4Y_B^2 Z_A^2 + \left(Z_A Y_0 + Y_A Z_0 - Y_B^2 Z_A Z_0\right)^2}$$

$$\Gamma_0 = \frac{Z_A^2 Y_0^2 - Z_0^2\left(Y_A - Y_B^2 Z_A\right)^2 + j\left(2Y_B Z_A\left(Z_A Y_0 - Y_A Z_0 + Y_B^2 Z_A Z_0\right)\right)}{4Y_B^2 Z_A^2 + \left(Z_A Y_0 + Y_A Z_0 - Y_B^2 Z_A Z_0\right)^2}$$

$$T_e = \frac{-4Y_B Z_A - 2j\left(Z_A Y_0 + Y_A Z_0 - Y_B^2 Z_A Z_0\right)}{4Y_B^2 Z_A^2 + \left(Z_A Y_0 + Y_A Z_0 - Y_B^2 Z_A Z_0\right)^2}$$

$$T_0 = \frac{4Y_B Z_A - 2j\left(Z_A Y_0 + Y_A Z_0 - Y_B^2 Z_A Z_0\right)}{4Y_B^2 Z_A^2 + \left(Z_A Y_0 + Y_A Z_0 - Y_B^2 Z_A Z_0\right)^2}$$

At the same time we can say that $B_1/V=S_{11}$, $B_2/V=S_{12}$, $B_3/V=S_{13}$ and $B_4/V=S_{14}$. Therefore s-parameters are:

$$s_{11} = \frac{\Gamma_e + \Gamma_0}{2}; s_{12} = \frac{T_e + T_0}{2}; s_{13} = \frac{T_e - T_0}{2}; s_{14} = \frac{\Gamma_e - \Gamma_0}{2}$$

And the scattering matrix of branch-line coupler is

$$[s] = \begin{bmatrix} s_{11} & s_{12} & s_{13} & s_{14} \\ s_{21} & s_{22} & s_{23} & s_{24} \\ s_{31} & s_{32} & s_{33} & s_{34} \\ s_{41} & s_{42} & s_{43} & s_{44} \end{bmatrix}$$

Matching Condition

Looking above equations if we consider the matching condition if $Z_A Y_0 = Z_0\left(Y_A - Y_B^2 Z_A\right)$ then s_{11} and s_{14} becomes zero. In that matching case, the power entering port 1 is evenly divided between ports 2 and 3 with a 90° phase shift between these output ports. No power is coupled to port 4 (isolated port).

Coupling, Directivity, Isolation and Power-split Ratio

As it can be seen from the matrix above that the scattering matrix of branch-line coupler is symmetric and each row of it is just the transpose of each column. Considering the coupling which is the ratio of power at port 1 to power at port 3, directivity which is the ratio of power at port 3 to power at port 4 and the isolation which is the ratio of power at port 1 to power at port 4 of the branch-line coupler:

Coupling = C = $10\log(P_1/P_3) = -20\log|S_{13}|$ dB

Directivity = D = $10\log(P_3/P_4) = -20\log(|S_{13}|/|S_{14}|)$ dB

Isolation = I = $10\log(P_1/P_4) = -20\log|S_{14}|$ dB

The power split ratio (P) which is used to express the coupling of the branch-line coupler in terms of the ratio of powers to the coupled (port 3) and direct ports (port 2) :

P = $10\log(P_3/P_2)=-20\log(|S_{13}|/|S_{12}|)$

Behavior of s-parameters versus frequency

In order to define the behavior of s-parameters with frequency, let us consider ABCD matrices of even and odd modes. In the previous section, in order to calculate s-parameters at the center frequency, we have taken βl as $\pi/2$ and therefore $\cos\beta l$ was 0 and $\sin\beta l$ was 1 ($\beta l=2\pi l/\lambda$ and $\lambda=v_p/f$). In this case since we will observe the dependence of s-parameters with respect to frequency, we will take $\sin\beta l$ and $\cos\beta l$ as they are and calculate s-parameters. Therefore,

$$\begin{bmatrix} A & B \\ C & D \end{bmatrix}_e = \begin{bmatrix} \cos\beta l - Z_A Y_B \sin\beta l & jZ_A \sin\beta l \\ j\left(Y_B\cos\beta l + Y_A \sin\beta l - Z_A Y_B^2 \sin\beta l - Y_B \cos\beta l\right) & \cos\beta l - Z_A Y_B \sin\beta l \end{bmatrix}$$

$$\begin{bmatrix} A & B \\ C & D \end{bmatrix}_o = \begin{bmatrix} \cos\beta l + Z_A Y_B \sin\beta l & jZ_A \sin\beta l \\ j\left(-Y_B\cos\beta l + Y_A \sin\beta l - Z_A Y_B^2 \sin\beta l - Y_B \cos\beta l\right) & \cos\beta l + Z_A Y_B \sin\beta l \end{bmatrix}$$

Solving for Γ_e, Γ_o, T_e, T_o:

Putting x for $\cos\beta l$ and y for $\sin\beta l$ in the equations;

$$\Gamma_e = \frac{j\left(Y_0 Z_A y - Z_0 Y_B x - Z_0 Y_A y + Z_0 Z_A Y_B^2 y - Z_0 Y_B x\right)}{\left(2x - 2Z_A Y_B y\right) + j\left(Z_A Y_0 y + Z_0 Y_B x + Z_0 Y_A y - Z_0 Z_A Y_B^2 y + Z_0 Y_B x\right)}$$

$$\Gamma_e = \frac{j\left(Y_0 Z_A y + Z_0 Y_B x - Z_0 Y_A y + Z_0 Z_A Y_B^2 y + Z_0 Y_B x\right)}{\left(2x + 2Z_A Y_B y\right) + j\left(Z_A Y_0 y - Z_0 Y_B x + Z_0 Y_A y - Z_0 Z_A Y_B^2 y - Z_0 Y_B x\right)}$$

$$\mathrm{T}_e = \frac{2}{\left(2x - 2Z_A Y_B y\right) + j\left(Z_A Y_0 y + Z_0 Y_B x + Z_0 Y_A y - Z_0 Z_A Y_B^2 y + Z_0 Y_B x\right)}$$

$$\mathrm{T}_e = \frac{2}{\left(2x + 2Z_A Y_B y\right) + j\left(Z_A Y_0 y - Z_0 Y_B x + Z_0 Y_A y - Z_0 Z_A Y_B^2 y - Z_0 Y_B x\right)}$$

At this point, if we use $s_{11} = \frac{\Gamma_e + \Gamma_0}{2}; s_{12} = \frac{\mathrm{T}_e + \mathrm{T}_0}{2}; s_{13} = \frac{\mathrm{T}_e - \mathrm{T}_0}{2}; s_{14} = \frac{\Gamma_e - \Gamma_0}{2}$, then we can get all the necessary s-parameters. After finding s-parameters, we can find magnitude of s-parameters and plot the magnitude versus frequency plot. This simulation program can plot the magnitude of s-parameters vs frequency.

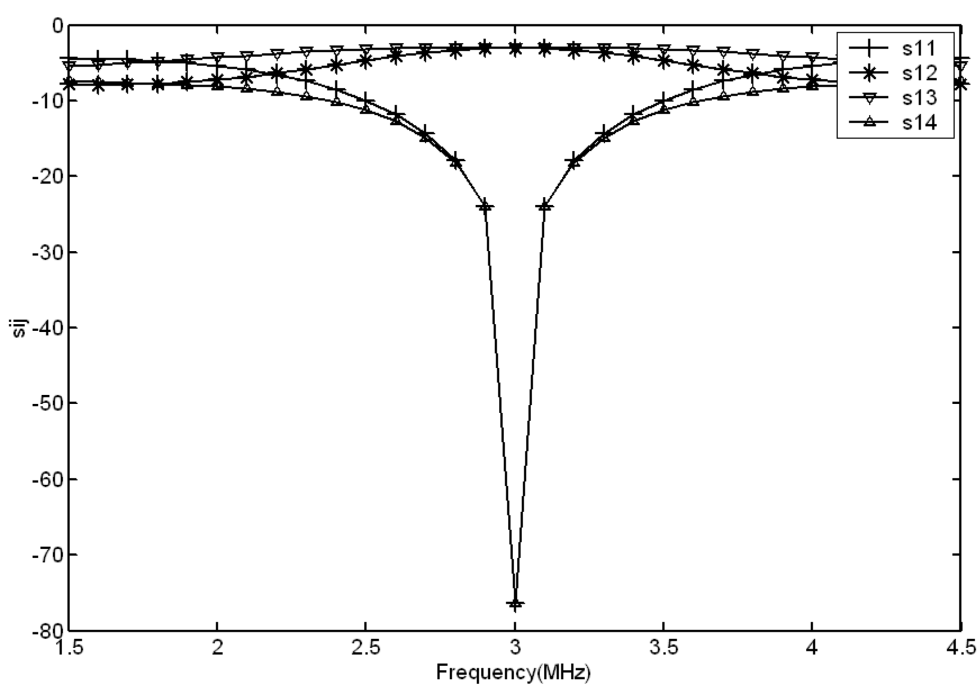

Figure 4.29 Scattering parameters for a branch line coupler

Usually $Z_B=Z_0$ and $Z_A=1/\sqrt{2}Z_0$ and the length of the horizontal as well as branch lines are chosen as $\lambda/4$, in that case we should have a very low isolation and reflection at the inputs and large value for the through and coupled output ports as depicted in Figure 4.29.

4.4 Ferrite Devices

4.4.1 Ferrite Devices

4.4.1.1 Electron movements

The magnetic property of any material is a result of electron movement within the atoms of the material. Electrons have two basic types of motion. The most familiar is the ORBITAL movement of the electron about the nucleus of the atom. Less familiar, but even more important, is the movement of the electron about its own axis, called ELECTRON SPIN. The different types of electron movement are illustrated in Figure 4.30.

1) Magnetic properties of material are due to magnetic dipole moments due to electron spin.
2) Most solids electron spin are in pairs and no net magnetic moments.
3) In magnetic materials large electron spins are unpaired but they are oriented in random directions and net magnetic moment is still small.
4) By applying steady (dc) external magnetic field $\mathbf{H_0}$, dipole moments align and large overall magnetic moment is realized (magnetization).
5) As $\mathbf{H_0}$ is increased more magnetic moments align with $\mathbf{H_0}$ and finally all of them align and it is in the saturation magnetization.
6) Ferrites are used in the saturated state.
7) Interaction of small ac microwave field **H** with the saturated ferrite material disturbs this stable state and a forced precession of the dipole moments around the $\mathbf{H_0}$ axis (analogous to precessing gyroscope in the earth's gravity) as depicted in Figure 4.31.

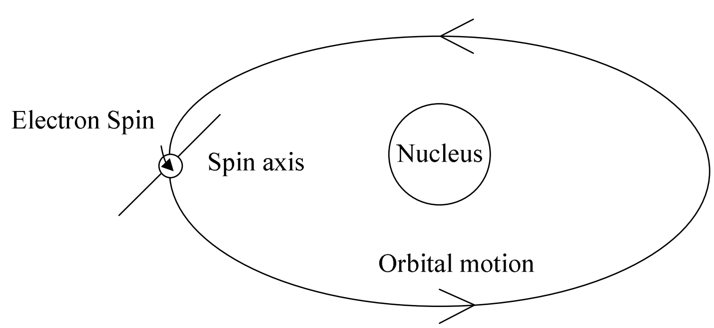

Figure 4.30 Two types of electron movement

You will recall that magnetic fields are generated by current flow. Since current is the movement of electrons, the movement of the electrons within an atom create magnetic fields. The magnetic fields caused by the movement of the electrons about the nucleus have little effect on the magnetic properties of a material. The magnetic fields caused by electron spin gives magnetic moments **m** and they combine to give material magnetic properties (**M**=N**m** where N is the number of effective spinning electrons per unit volume and **M** is the magnetization). In most materials the spin axes of the electrons are so randomly arranged that the magnetic fields largely cancel out and the material displays no significant magnetic properties. The electron spin axes in some materials, such as iron and nickel, can be caused to align by applying an external steady magnetic field $\mathbf{H_o}$. With the steady magnetic field application, **m** precess gyromagnetically around $\mathbf{H_o}$ due to torque $\boldsymbol{\tau} = \mathbf{m} \times \mu \mathbf{H_o}$ The direction of precession is determined by $\mathbf{H_0}$ and is clockwise looking along $\mathbf{H_0}$ as shown in Figure 4.31. The angle of precession θ between $\mathbf{H_0}$ and **m** decrease due to friction and the ferrite is magnetized with the magnetic momentum **M** when electron spins are aligned with $\mathbf{H_0}$.

The alignment of the electrons within a material causes the magnetic fields to add, and the material then has magnetic properties. In the absence of an external force, the axis of any spinning object tends to remain pointed in one direction. Spinning electrons behave the same way. Therefore, once the electrons are aligned, they tend to remain aligned even when the external field is removed. The orbital motion of the electrons about the nucleus and the force that holds the atom together causes electron alignment in a ferrite. When a static magnetic field is applied, the electrons try to align their spin axes with the new force. The attempt of the electrons to balance between the interaction of the new force and the binding force causes the electrons to wobble (literal meaning to move or proceed with an irregular rocking or staggering motion or unsteadily and clumsily from side to side) on their axes, as shown in Figure 4.31. The wobble of the electrons has a natural resonant WOBBLE FREQUENCY that varies with the strength of the applied field. Ferrite action is based on this behavior of the electrons under the influence of an external field and the resulting wobble frequency.

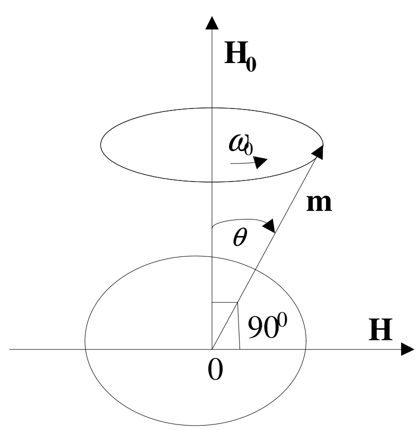

Figure 4.31 Precessing of electron in a steady magnetic field

Digression: Polarization

For a TEM wave propagating along z-axis, we can write: $\mathbf{E} = (E_1\hat{x} + E_2\hat{y})e^{-jk_0 z}$ and we can consider the following particular cases:

1. $E_1 \neq 0$ and $E_2 = 0$, a plane linearly polarized in x-axis

2. $E_1 = 0$ and $E_2 \neq 0$, a plane linearly polarized in y-axis
3. $E_1 \neq 0$ and $E_2 \neq 0$, a plane linearly polarized in $\varphi = \tan^{-1}\frac{E_2}{E_1}$
4. $E_1 = E_2 \neq 0$, a plane linearly polarized in $\varphi = 45^0$

As we know that for linearly polarized waves, electric field vector keeps pointing in a fixed direction.

5. $E_1 = jE_2 = E_0$

$$\mathbf{E} = E_0(\hat{x} - j\hat{y})e^{-jk_0 z}; \mathbf{E}(z,t) = E_0\left(\hat{x}\cos(\omega t - k_0 z) + \hat{y}\cos\left(\omega t - k_0 z - \frac{\pi}{2}\right)\right)$$

For fixed position say z=0, the time domain form of the field reduces to

$$\mathbf{E}(z,t) = E_0(\hat{x}\cos\omega t + \hat{y}\sin\omega t); \varphi = \tan^{-1}\frac{\sin\omega t}{\cos\omega t} = \omega t$$

So as ωt increases from zero, the electric field vector rotates in counter clockwise from the x-axis (RHCP) and the polarization rotates at the uniform angular velocity ω. Similarly for LHCP, $\mathbf{E} = E_0(\hat{x} + j\hat{y})e^{-jk_0 z}$ the polarization rotates clockwise at the uniform angular velocity ω. Besides any linearly polarized wave can be expressed as a combination of RHCP and LHCP. $\mathbf{E} = \hat{x}E_0 e^{-jk_0 z} = \left[\frac{E_0}{2}(\hat{x} + j\hat{y}) + \frac{E_0}{2}(\hat{x} - j\hat{y})\right]e^{-jk_0 z}$

4.4.1.2 Propagation of Microwaves in Ferrites

The propagation characteristics of microwaves in ferrites are exploited for applications in non-reciprocal microwave devices. Ferrite is a family of $MeO.Fe_2O_3$ where Me is a divalent iron metal (Cobalt, Nickel, Zinc, Mangnese, Cadmium, etc). The specific resistance of ferrites is very high (≈10^{14} times as high as those of metals), relative permittivity of 10-15 and low loss tangent tanδ =10^{-14} at microwave frequencies. Ferrite is nonlinear material and its permeability is an asymmetric tensor (when the bias magnetic field $\mathbf{H_0}$ is along z-axis) is expressed as

$$\mathbf{B} = \tilde{\boldsymbol{\mu}}\mathbf{H} \Rightarrow \begin{bmatrix} B_x \\ B_y \\ B_z \end{bmatrix} = \begin{bmatrix} \mu_{xx} & \mu_{xy} & \mu_{xz} \\ \mu_{yx} & \mu_{yy} & \mu_{yz} \\ \mu_{zx} & \mu_{zy} & \mu_{zz} \end{bmatrix}\begin{bmatrix} H_x \\ H_y \\ H_z \end{bmatrix}; \tilde{\boldsymbol{\mu}} = \begin{bmatrix} \mu & jk & 0 \\ -jk & \mu & 0 \\ 0 & 0 & \mu_0 \end{bmatrix}$$

where μ is the diagonal susceptibility and k is the off-diagonal elements. The relative permeabilities of ferrites are of order few thousands. Ferrites are dielectrics but exhibit magnetic anisotropy: (a) the transmission coefficient for microwave propagation through ferrite is not the same for different directions (b) non-reciprocal rotation of the plane of polarization.

If we apply a steady external magnetic field $\mathbf{H_0}$ then for anti-clockwise (along $\mathbf{H_0}$ direction) and clockwise polarization (along $\mathbf{H_0}$ direction) of wave propagation there will be different propagation constants

$$\beta^+ = \omega\sqrt{\varepsilon\mu^+} = \frac{2\pi}{\lambda^+}; \beta^- = \omega\sqrt{\varepsilon\mu^-} = \frac{2\pi}{\lambda^-}; \mu_+ = \mu_+^{'} - j\mu_+^{''}; \mu_- = \mu_-^{'} - j\mu_-^{''}$$

where the superscript "+" is for anti-clockwise polarization and superscript "–" for clockwise polarization. Therefore for a linearly polarized wave propagating along the direction of H_0 the plane of polarization rotates and it is non-reciprocal. The rotation of electric field of linearly polarized wave passing through a magnetized ferrite material is called as FARADAY ROTATION. Let a linearly polarized wave propagate in ferrite along z-axis at z=0. Since the linearly polarized wave can be decomposed into anti-clockwise and clockwise circularly polarized waves. These components propagate with different propagation constants β^+ and β^- respectively and the corresponding waves rotate at different rates. Over a distance of z, the resultant linearly polarized wave will experience a phase delay and this property is exploited in ferrite isolators and circulators. A microwave signal circularly polarized in the same direction, as the precession will interact strongly with dipole moments while oppositely polarized wave will interact less strongly. A microwave signal will propagate through a ferrite differently in different directions due to this polarization sensitivity (β^+ for RHCP and β^- for LHCP).

$$\mathbf{E} = \left[\frac{E_0}{2}(\hat{x} + j\hat{y})e^{-j\beta^+ z} + \frac{E_0}{2}(\hat{x} - j\hat{y})e^{-j\beta^- z}\right]$$
$$= \frac{E_0}{2}\hat{x}\left(e^{-j\beta^+ z} + e^{-j\beta^- z}\right) - j\frac{E_0}{2}\hat{y}\left(e^{-j\beta^+ z} - e^{-j\beta^- z}\right)$$
$$= E_0\left[\hat{x}\left(\cos\left(\frac{\beta^+ - \beta^-}{2}\right)z\right) - \hat{y}\left(\sin\left(\frac{\beta^+ - \beta^-}{2}\right)z\right)\right]e^{-j\frac{\beta^+ + \beta^-}{2}z}$$

Hence

$$\varphi = \tan^{-1}\frac{E_y}{E_z} = -\left(\frac{\beta^+ - \beta^-}{2}\right)z$$

Thus polarization is rotated through the angle φ and it is called Faraday rotation. Note that the derivation of the above formula in ferrite loaded waveguide is a bit involved and it is not very difficult also. This can be done using the following source-free Maxwell equations in ferrites:

$$\nabla \times \mathbf{E} = -j\omega[\mu]\mathbf{H}; \nabla \times \mathbf{H} = j\omega\varepsilon\mathbf{E}$$

and applying the boundary conditions will lead us to the following equation:

$$\beta^{+} - \beta^{-} \cong \frac{2k_c k\Delta S}{\mu S}\sin 2k_c x_0; k_c = \frac{\pi}{a}; \frac{\Delta S}{S} = \frac{w}{a}$$

where the ferrite is placed in the waveguide for $x=x_0,x_0+w$ (refer to Figure 13.3), k_c is the cut-off frequency of empty waveguide, ΔS/S is the filling factor and the result is accurate for any type of waveguide with ΔS/S<0.01. Note that k is the off-diagonal elements and μ is the diagonal components of permeability tensor.

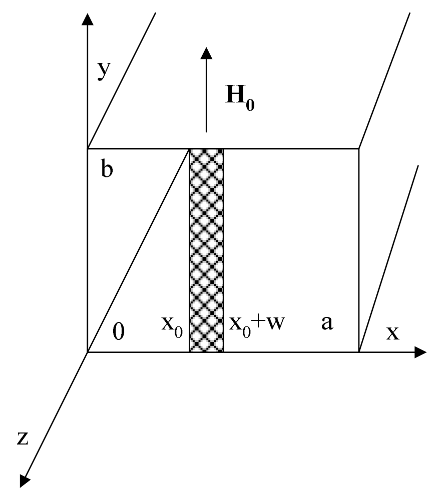

Figure 4-32 Ferrite loaded waveguide

FERRITE ISOLATORS An isolator is a non-reciprocal transmission device that is used to isolate one component from reflections of other components. An ideal isolator completely absorbs the power of propagation in one direction and provides loss less transmission in the other direction. Isolators are generally used to improve the stability of microwave generators such as klystron and magnetrons in which the reflections from the load affects the generating frequency. In such cases, isolator placed between the generator and load prevents the reflected power from the mismatched load from returning to the generator. An isolator is a ferrite device that can be constructed so that it allows microwave energy to pass in one direction but blocks energy in the other direction in a waveguide.

GYRATOR

FERRITE CIRCULATORS

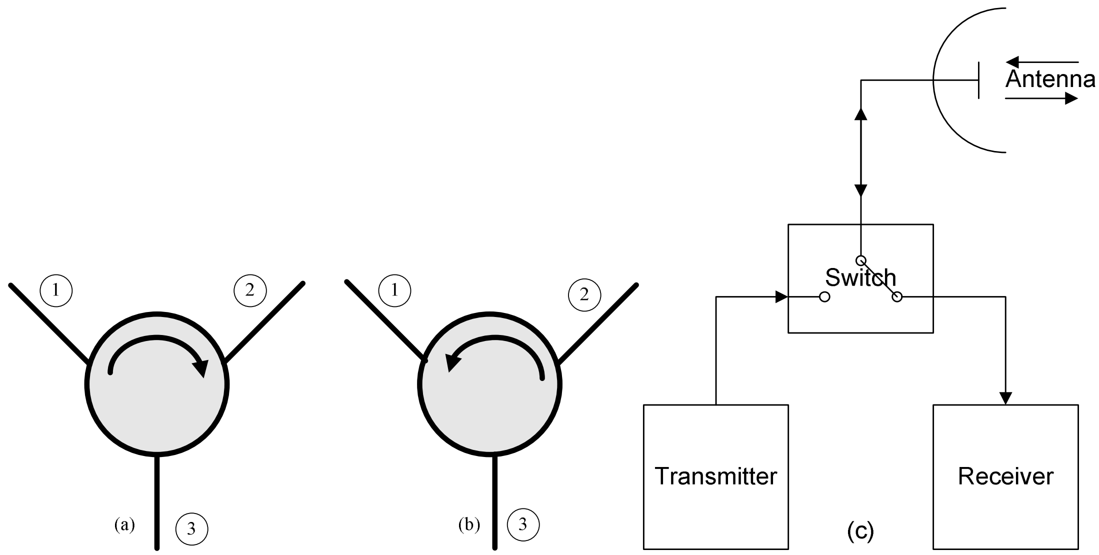

Figure 4.33 Ferrite circulator: (a) clock-wise (b) anti-clockwise (c) Diplexer switch in active antenna systems

Scattering matrix representations of circulators:

$[s]=\begin{bmatrix}0 & 0 & 1\\ 1 & 0 & 0\\ 0 & 1 & 0\end{bmatrix}$ for clockwise circulator of Figure 4.33 (a) and $[s]=\begin{bmatrix}0 & 1 & 0\\ 0 & 0 & 1\\ 1 & 0 & 0\end{bmatrix}$ for anti-clockwise circulator of Figure 4.33 (b). Note that if we terminate one port of the circulator, it becomes an isolator. For a loss less, small mismatched Γ circulator of Figure 4.33 (a), we have,

$$[s]=\begin{bmatrix}\Gamma & \beta & \alpha\\ \alpha & \Gamma & \beta\\ \beta & \alpha & \Gamma\end{bmatrix}.$$

Since the device is loss less, scattering matrix is unitary. $|\Gamma|^2+|\alpha|^2+|\beta|^2=1;\Gamma\beta^*+\alpha\Gamma^*+\beta\alpha^*=0$. For small mismatched case, $|\Gamma|<<1$, $|\beta|<<1$, $|\alpha|\approx 1$, then $\alpha\Gamma^*+\beta\alpha^*\approx 0\Rightarrow|\Gamma|=|\beta|$ and $2|\Gamma|^2+|\alpha|^2=1\Rightarrow|\alpha|\approx 1-|\Gamma|^2$. Therefore,

$$[s]=\begin{bmatrix}\Gamma & \Gamma & 1-|\Gamma|^2\\ 1-|\Gamma|^2 & \Gamma & \Gamma\\ \Gamma & 1-|\Gamma|^2 & \Gamma\end{bmatrix}$$

Ferrite circulators are often used as a diplexer as depicted in Figure 4.33 (c) generally in modules for active antennas (whenever a single antenna is used for both transmitting and receiving, as in a radar system, an electronic switch must be used, switching systems of this type are called diplexers). The operation of a circulator can be compared to a revolving door with three entrances and one mandatory rotating sense. This rotation is based on the interaction of the electromagnetic wave with magnetized ferrite. A microwave signal entering via one specific port follows the prescribed rotating sense and has to leave the circulator via the next port and so on. Energy from the transmitter rotates anticlockwise to the antenna port. Virtually all circulators used in radar applications contain ferrite. By the symmetric construction of the ferrite circulator it is always possible to determine a defined way of direction by the choice of connection.

Note that additional materials will be discussed in the class for ferromagnetic devices and this lecture note is incomplete. Besides PCML filter material will be provided for additional reading (PCML filter not included for examination).

Review Question 4.6 Ferrite devices are useful in microwave applications because of _____ properties.
Review Question 4.7 Rotating the plane of polarization of a wave front by passing it through a ferrite device is known as _____.

REFERENCES
Periodic structures:
1. R. S. Kshetrimayum and L. Zhu, Hybrid MoM-Immittance Approach for full-wave characterization of printed strips and slots in layered waveguide and its applications," *IEICE Trans. Electron.*, vol.-E87-C, no. 5, pp. 700-707, May 2004.
2. R. E. Collin, *Field theory of guided waves*, IEEE Press, New York, 1991.
3. R. S. Kshetrimayum, *Printed periodic waveguide structures*, VDM Verlag, Germany, 2009.

Filters:
1. R. Levy, R.V. Snyder and G. Matthaei, "Design of Microwave Filters," *IEEE Transactions on Microwave Theory and Techniques*, Vol. 50, No. 3, Mar. 2002, pp. 783-793.
2. D. M. Pozar, *Microwave Engineering*, 3rd Edition, John Wiley and Sons, New York, 2005.
3. G. L. Matthaei, L. Young and E. M. T. Jones, Microwave filters, Impedance-matching networks, and coupling structures, Artech House, MA, 1980.

Power dividers and couplers:
1. S. M. Liao: Microwave Devices and Circuits, PHI, 1995, 3/e
2. D. M. Pozar: Microwave Engineering, John Wiley, 2005, 3/e
3. A. Das and S. K. Das, Microwave Engineering, Tata McGraw-Hill, 2005, 1/e

Ferrimagnetic devices:
1. S. M. Liao: Microwave Devices and Circuits, PHI, 1995, 3/e
2. R. E. Collin: Foundation for Microwave Engineering, John Wiley, 2005, 2/e
3. A. Das and S. K. Das, Microwave Engineering, Tata McGraw-Hill, 2005, 1/e